



# ***Computational-Experimental Study of Plasma Processing of Carbides at High Temperatures***

**Arturo Bronson and Vinod Kumar**  
**Department of Mechanical Engineering**  
**University of Texas at El Paso**

**Program Manager: Richard J. Dunst**  
**National Energy Technology Laboratory**  
**DOE Award – FE0008400**



# **High Temperature Research Group**

- **Graduate Students**
  - **Alejandro Garcia (Computational - Masters) to Delfingen Inc.**
  - **Arturo Medina (Computational - Masters)\***
  - **Sanjay Shantha-Kumar (Experiment - Ph.D.)\***
- **Senior/Graduate Student Transition**
  - **Alberto Delgado (Experimental/Computational – Dual B. S. in Mechanical Engineering with B. S. in Metallurgical & Materials Engineering, MME); Now pursuing MS in MME.**

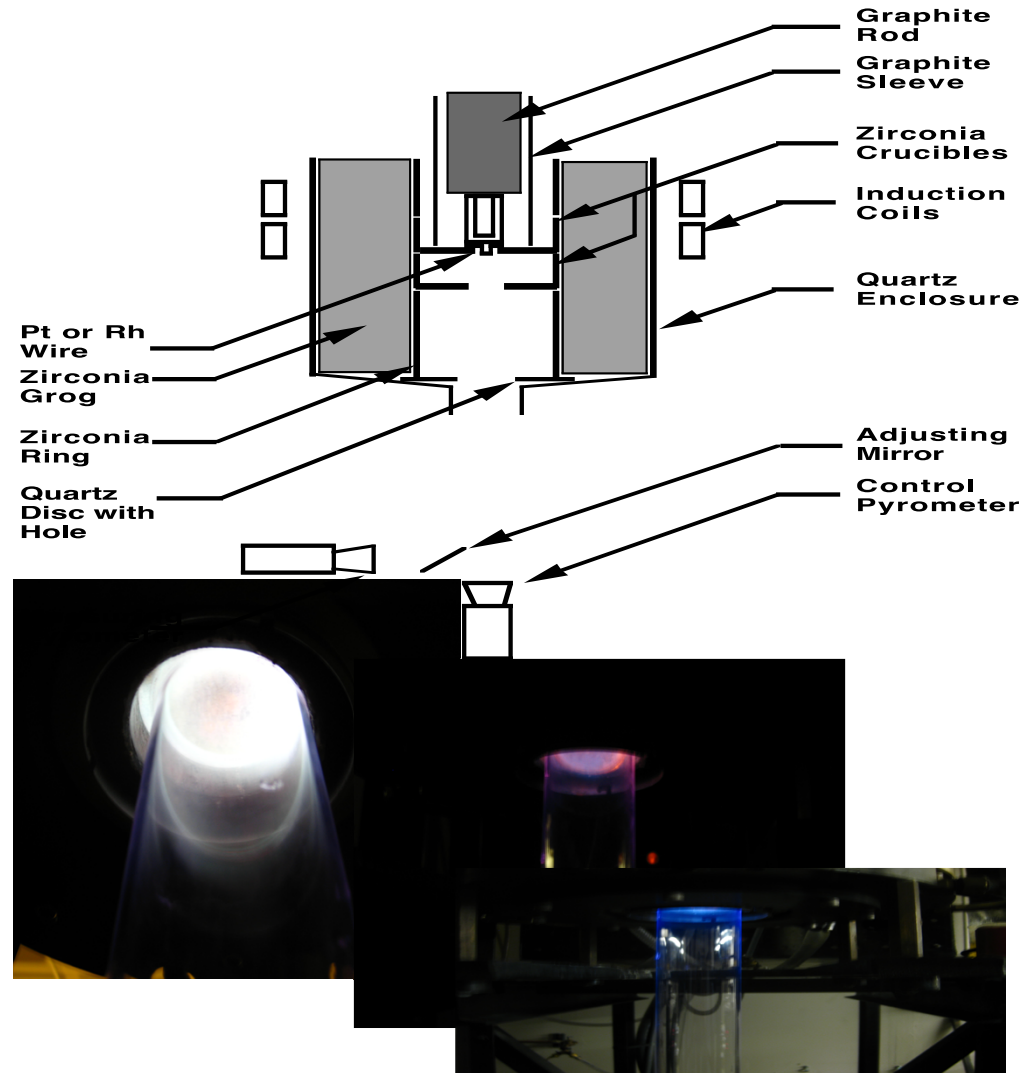
---

**\* Aids students in high temperature research.**



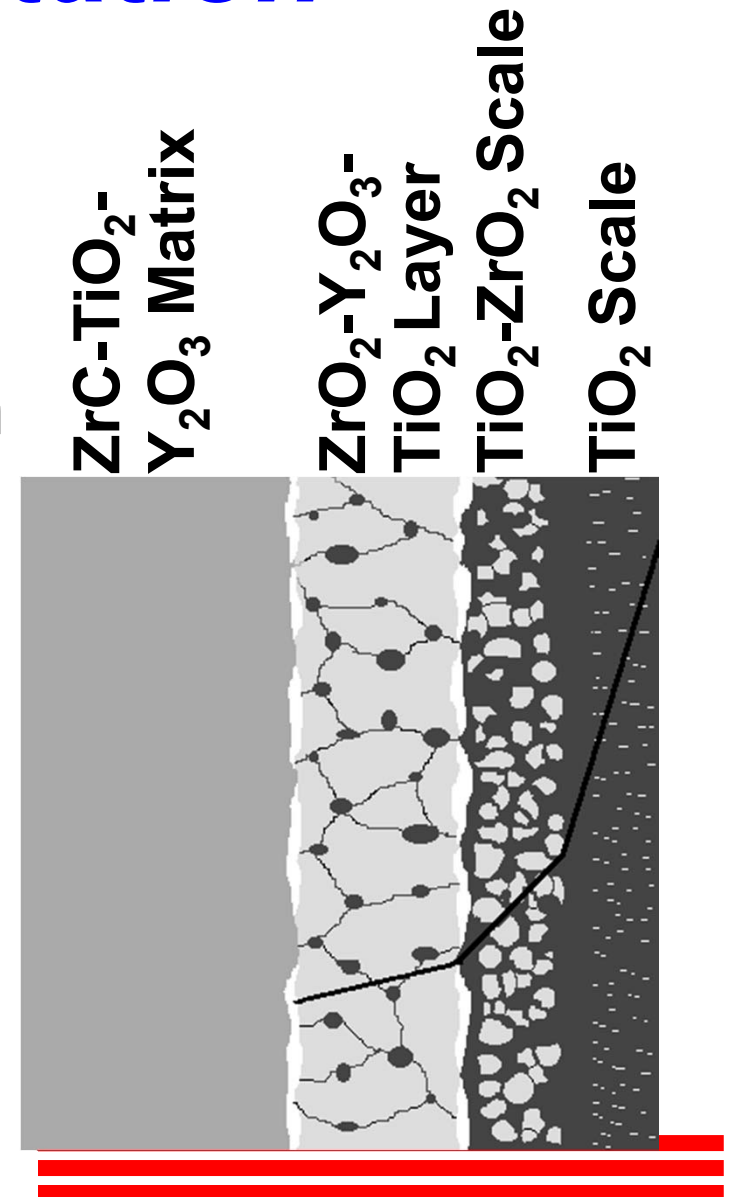
# **Motivation/Impact of Research**

- Use electromagnetics to **control plasma surface reactions.**
- Use plasma processing to **create temperature extremes.**
- Use temperature spikes to **form metastable phases.**
- Use electromagnetics to **change diffusional flux.**



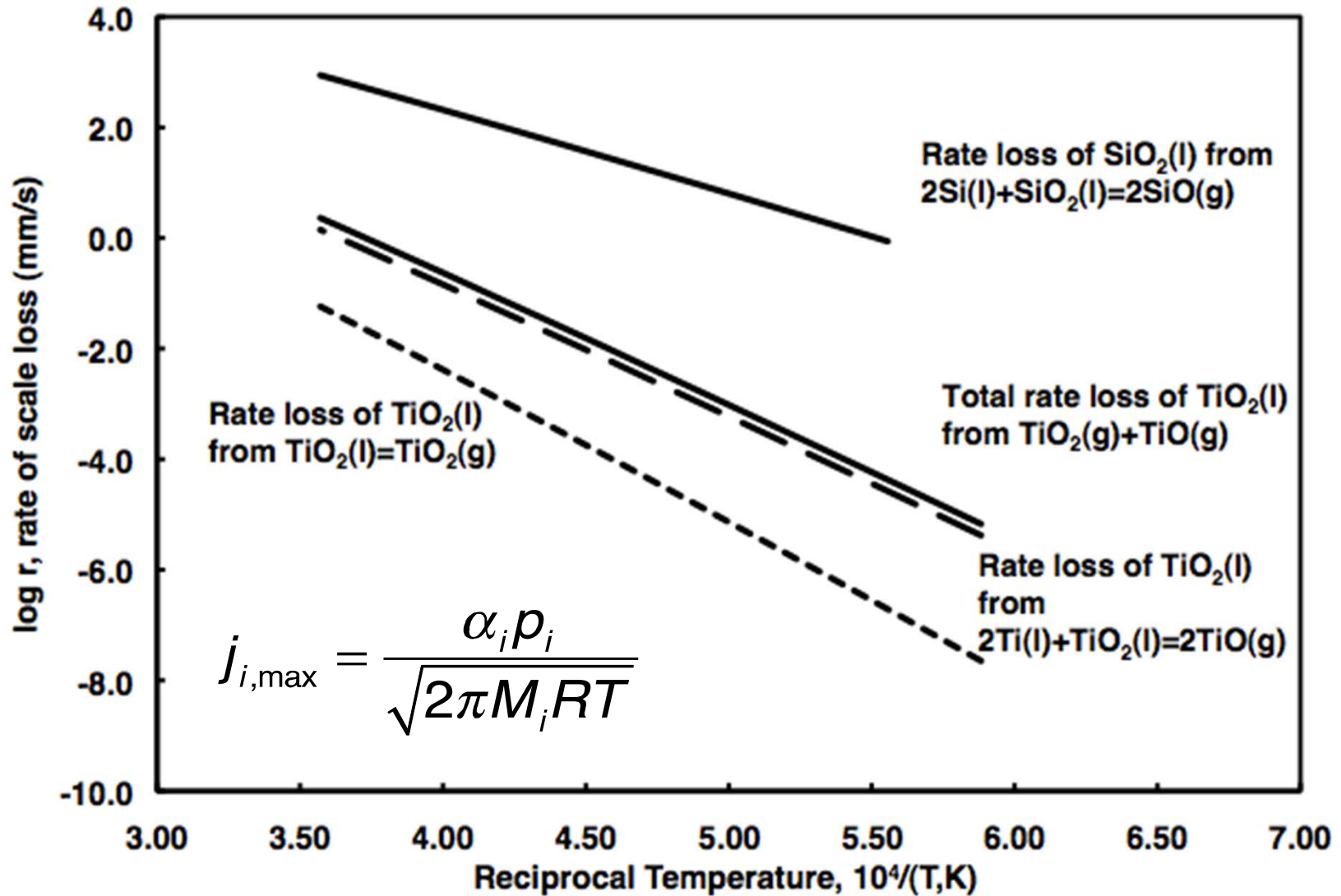
# *Outline of Presentation*

- Introduction – Processing
  - Scale of  $\text{Al}_2\text{O}_3$  and  $\text{TiO}_x$
  - Plasma Surface Reactions
- **Computational thermodynamics** coupled with heterogeneous kinetics **infused with fluid dynamics** to model plasma gas reactions
- Strategic Experimentation –  $\text{Ti}_3\text{AlC-TiC}$  Processing and Oxidation
- Analysis of Plasma-Surface Reactions



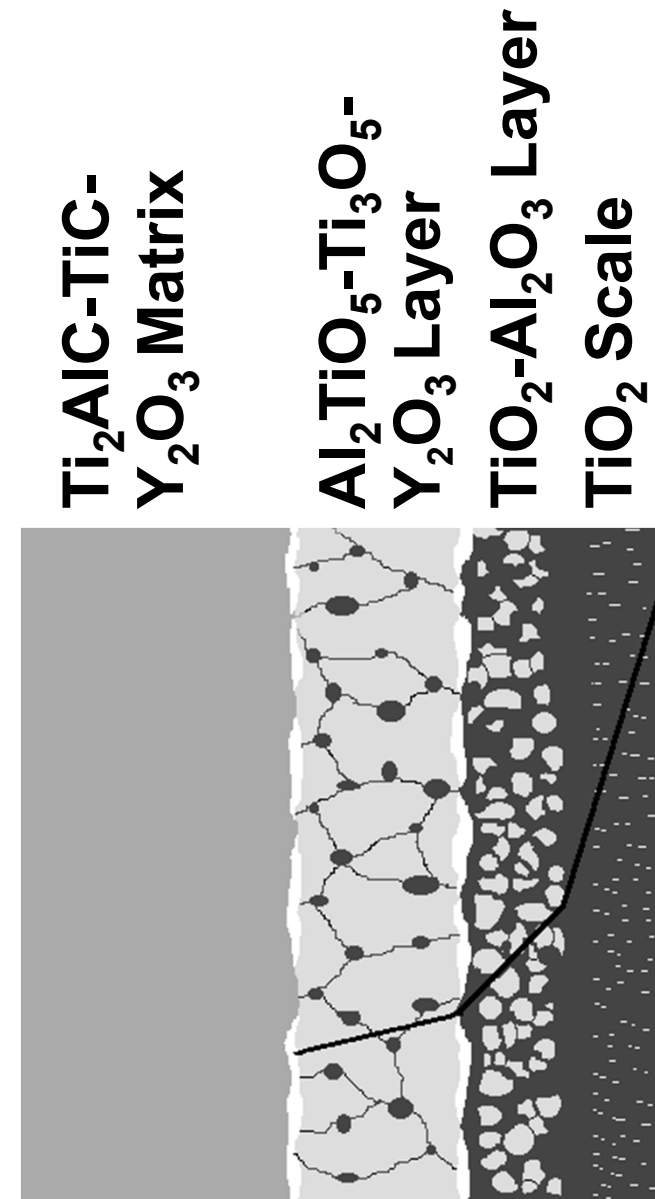


# Vaporizing Flux of $\text{SiO}_2$ and $\text{TiO}_2$



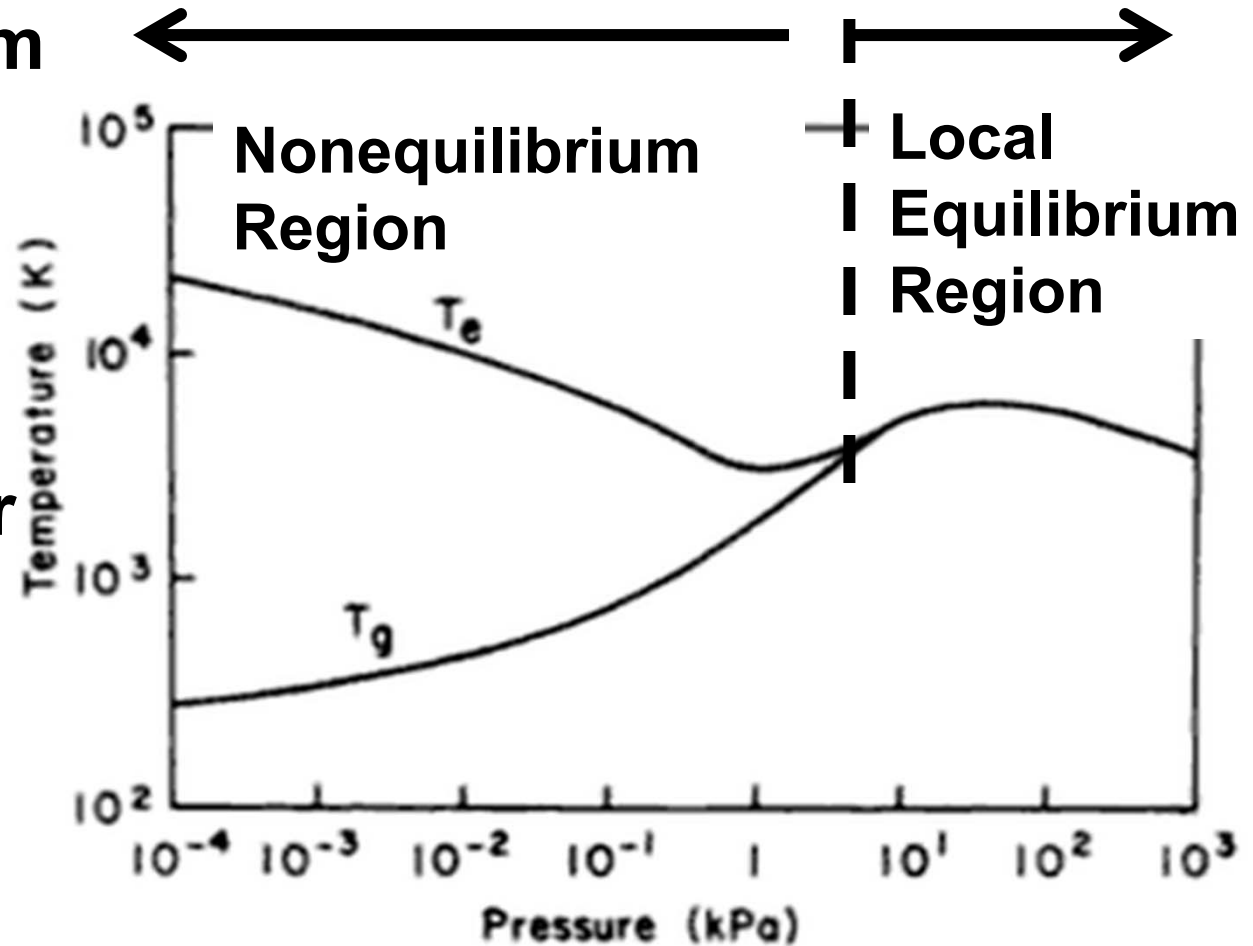
# Project Objectives

- Investigate the effects of **plasma surface reactions within pores of carbide packed bed**;
- Investigate the plasma-surface reactions on high temperature carbides
- Investigate the **effect of the potential gradients of the electromagnetic field** on mass transfer



# Plasma Temperatures - Pressures

- Non-equilibrium versus local equilibrium plasmas
- Plasma energy in terms of  $T$  or  $(T_e - T_g)/T_e$
- Significantly lower number of studies on plasma-surface reactions.

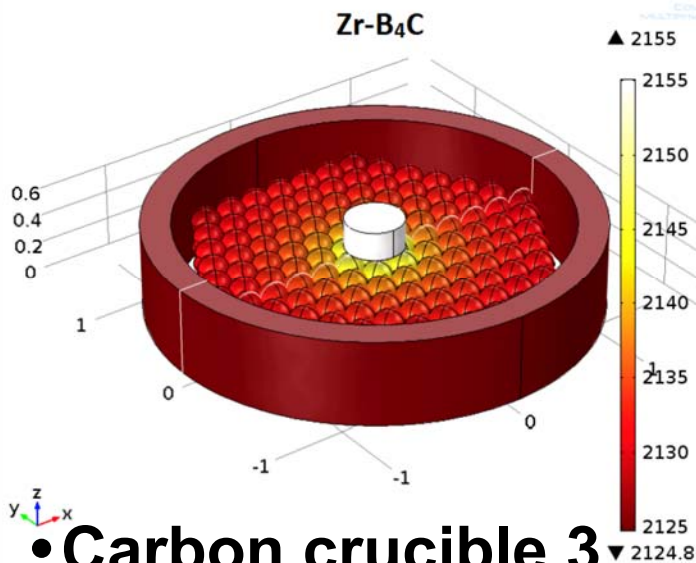


Boulous, Fauchais and Pfender--1994

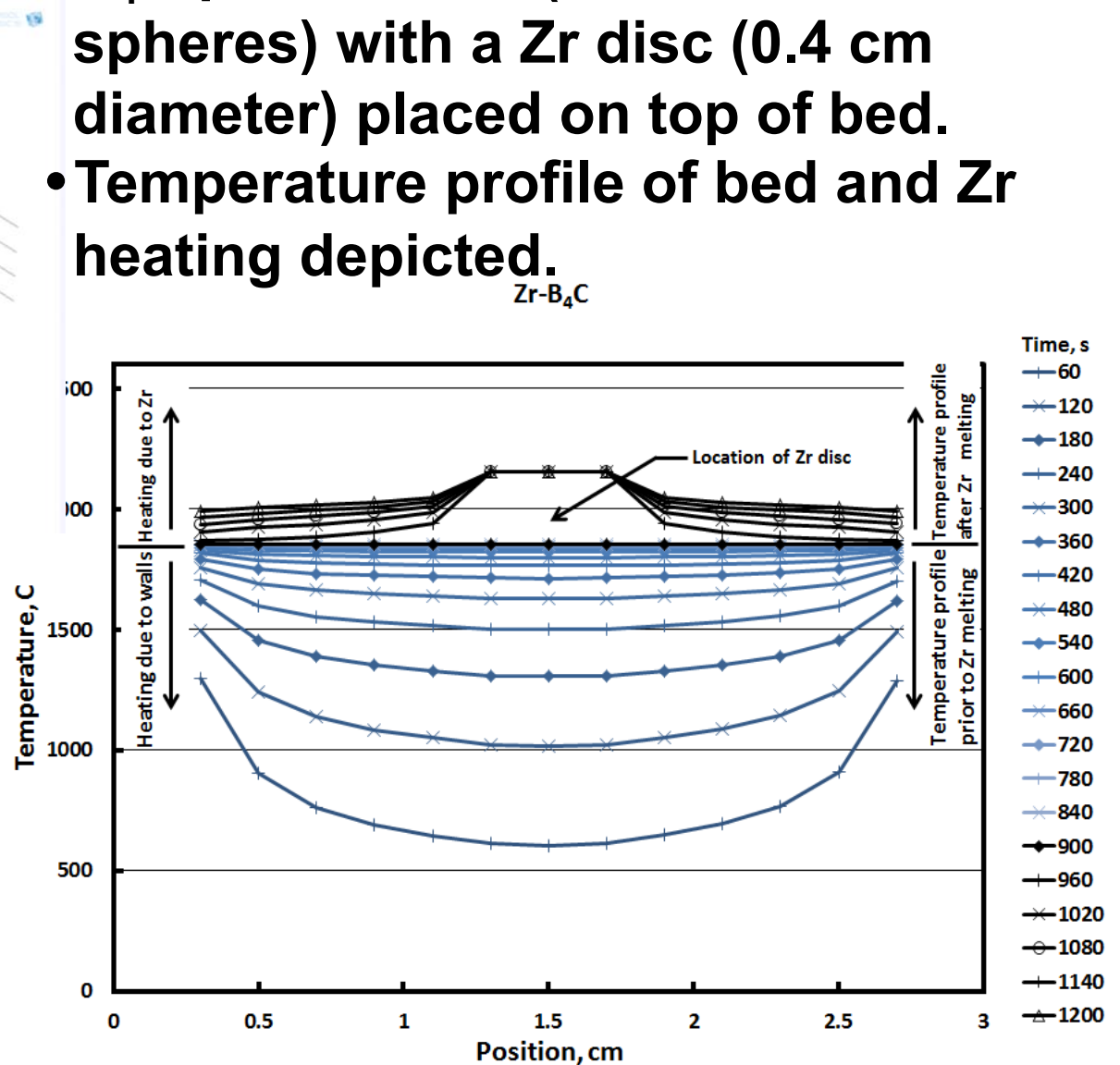


# Temperature Transients from COMSOL Simulations

- $B_4C$  packed bed (0.2 cm diameter spheres) with a Zr disc (0.4 cm diameter) placed on top of bed.
- Temperature profile of bed and Zr heating depicted.



- Carbon crucible 3 cm OD-2.6 cm ID & 254  $B_4C$  spheres.
- $B_4C$  melts at  $2450^\circ C$
- Zr melts at  $1855^\circ C$
- $k_{B_4C}=4.5$ ,  $k_{Zr}=34$  W/(mK)

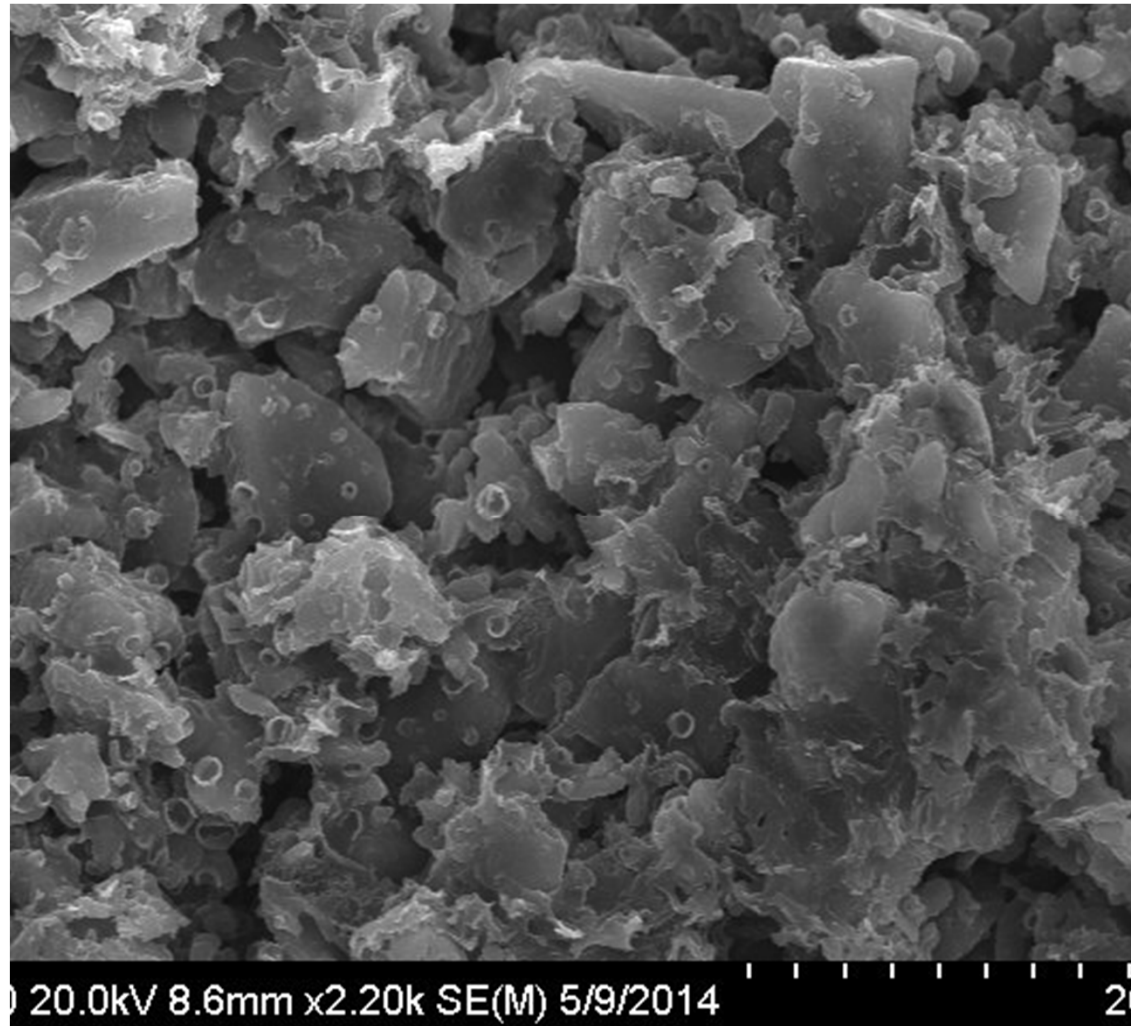






## ***B<sub>4</sub>C Microstructure after 1700° C Heating***

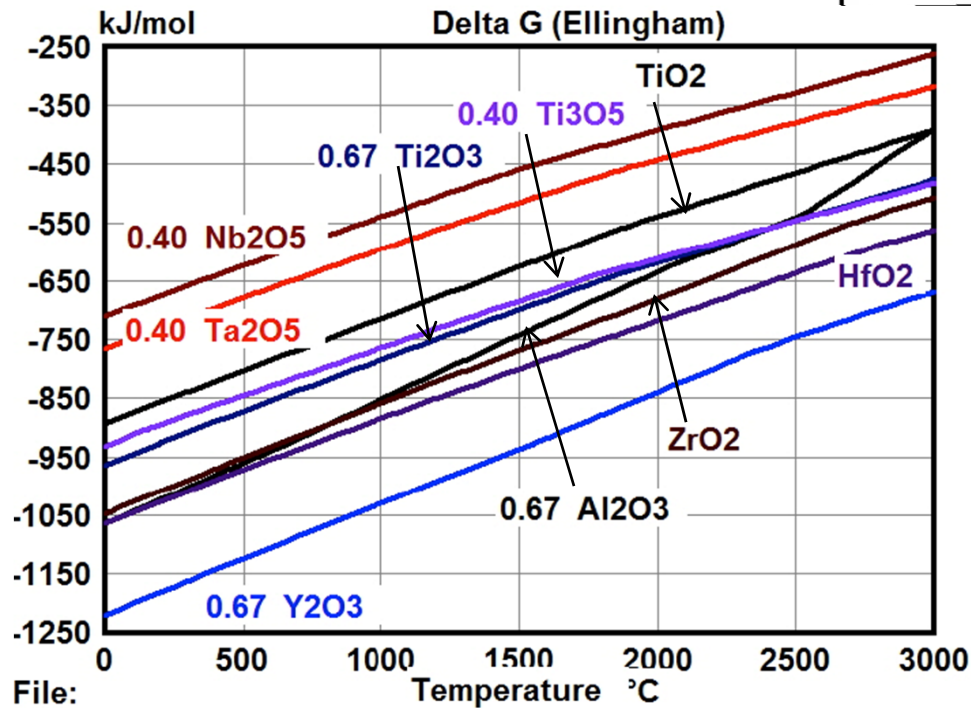
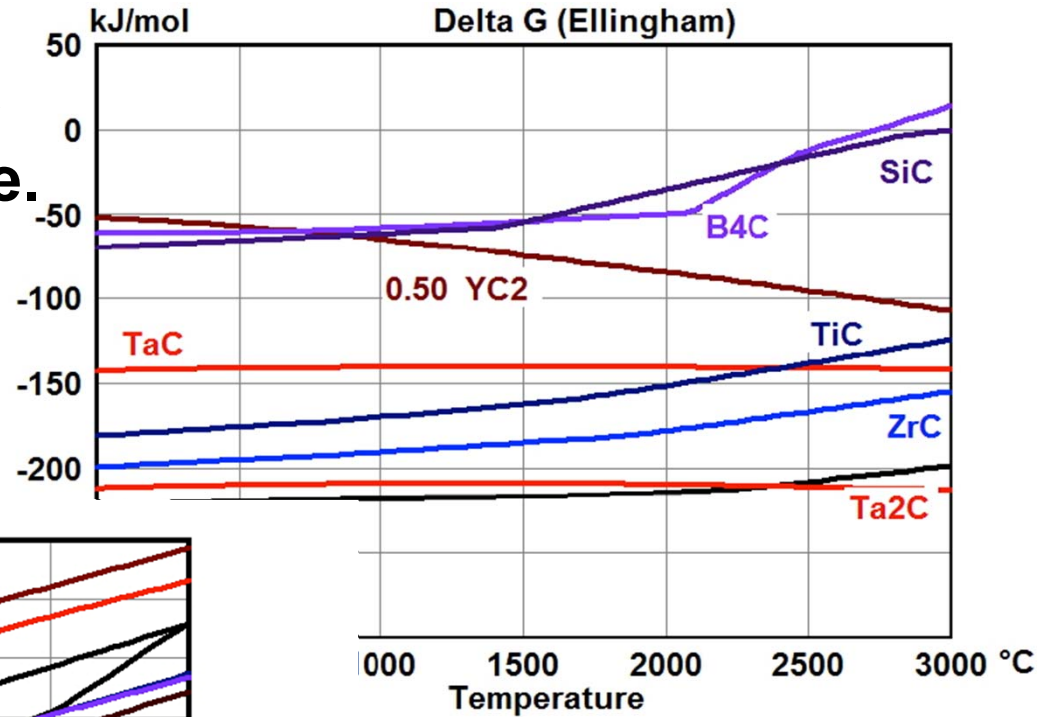
- B<sub>4</sub>C powder averaging 10 μm was heated to 1700° C in a graphite crucible.
- Afterwards, liquid Bi was used to embed particles followed by polishing.
- Pores vary from 1 to 10 μm.





# Stabilities-Oxides and Carbides

- For carbides, HfC, Ta<sub>2</sub>C and ZrC are most stable.
- For oxides, Y<sub>2</sub>O<sub>3</sub> and HfO<sub>2</sub> are most stable.
- Used Outotec HSC v. 7



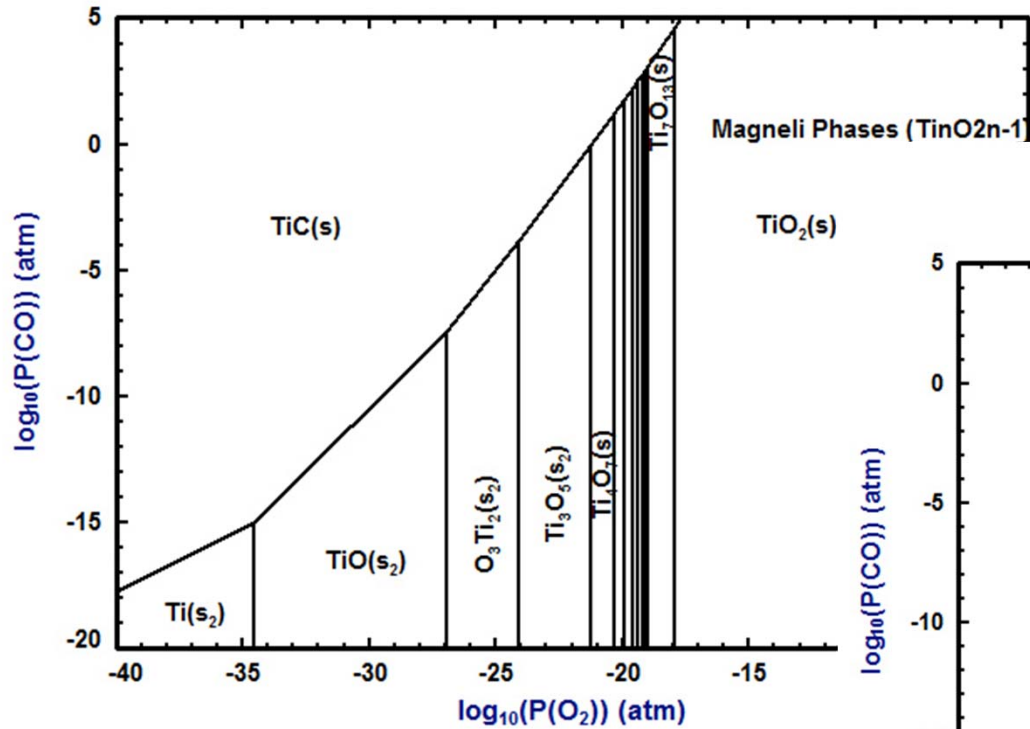
File:



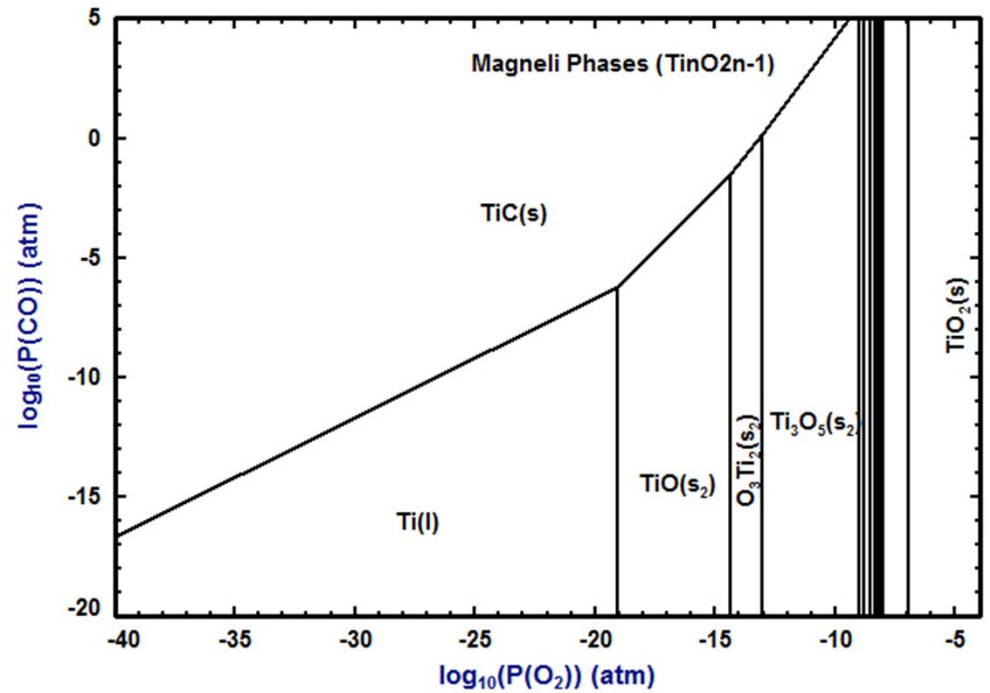


# Ti-C-O Stability Diagrams at 1273 & 1973K for Expanded View of Magneli phases & $p_{O_2}$

Ti-C-O, 1273 K

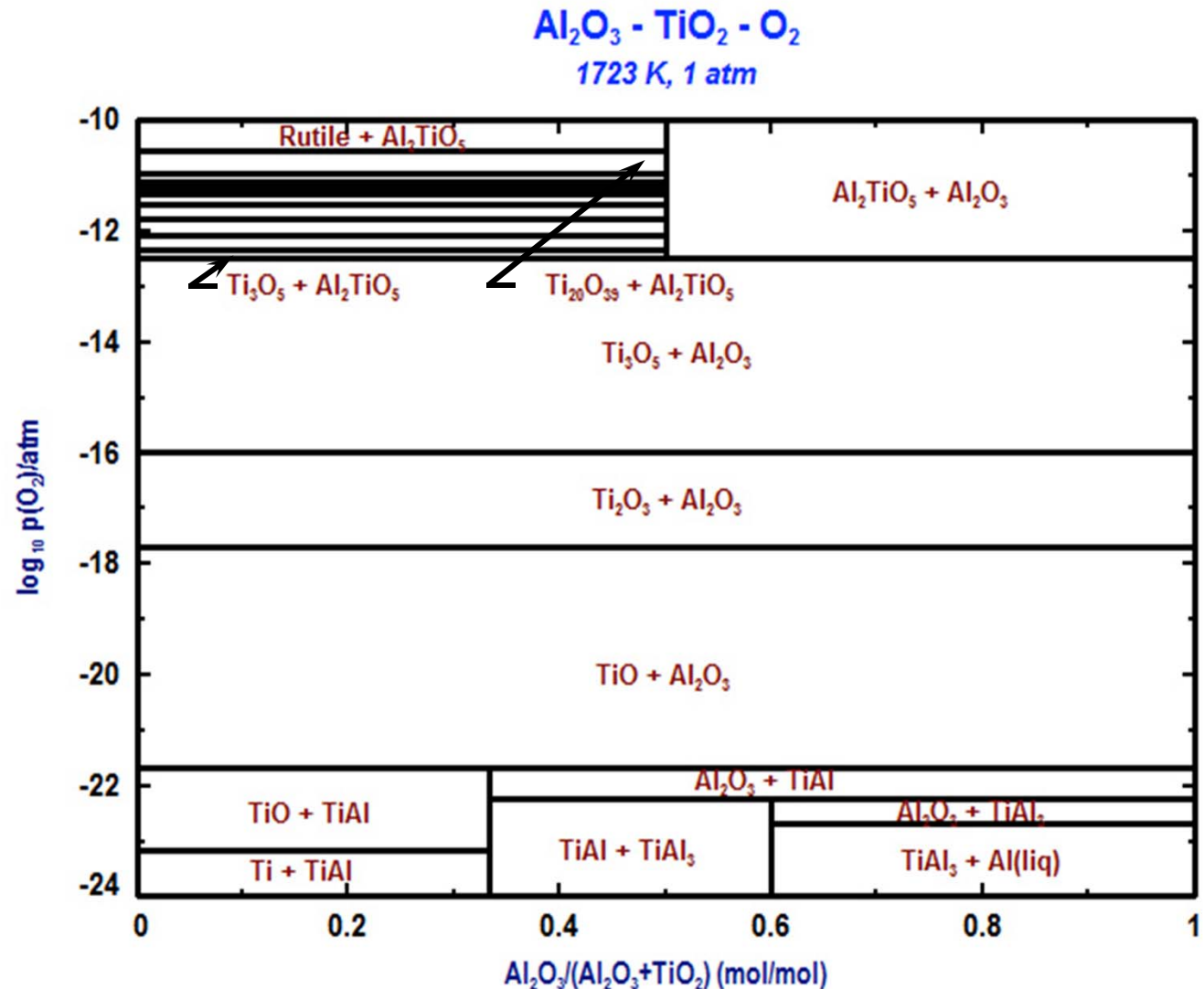


Ti-C-O, 1973 K



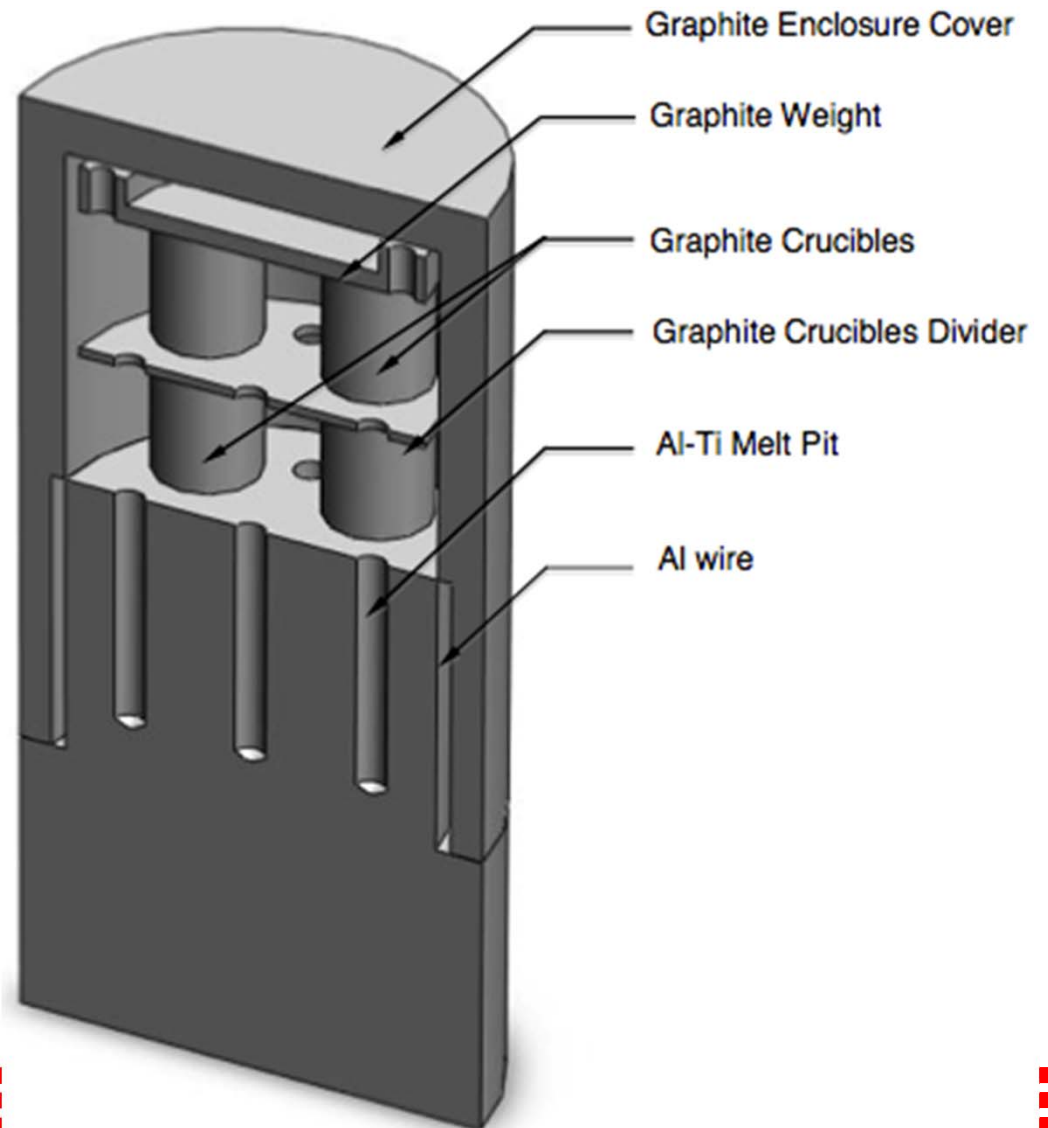
# Possible Scale of Oxidized $Ti_2AlC-TiC$

- Ti oxides depend on  $pO_2$  level within scale.
- Muan/Osborn showed limited solubility of  $Al_2O_3 - Al_2O_3 \cdot TiO_2$  and  $Al_2O_3 \cdot TiO_2 - TiO_2$  pseudobinaries.
- $Al_2O_3 \cdot TiO_2$  melts congruently at  $1860^\circ C$  as per Muan/Osborn.

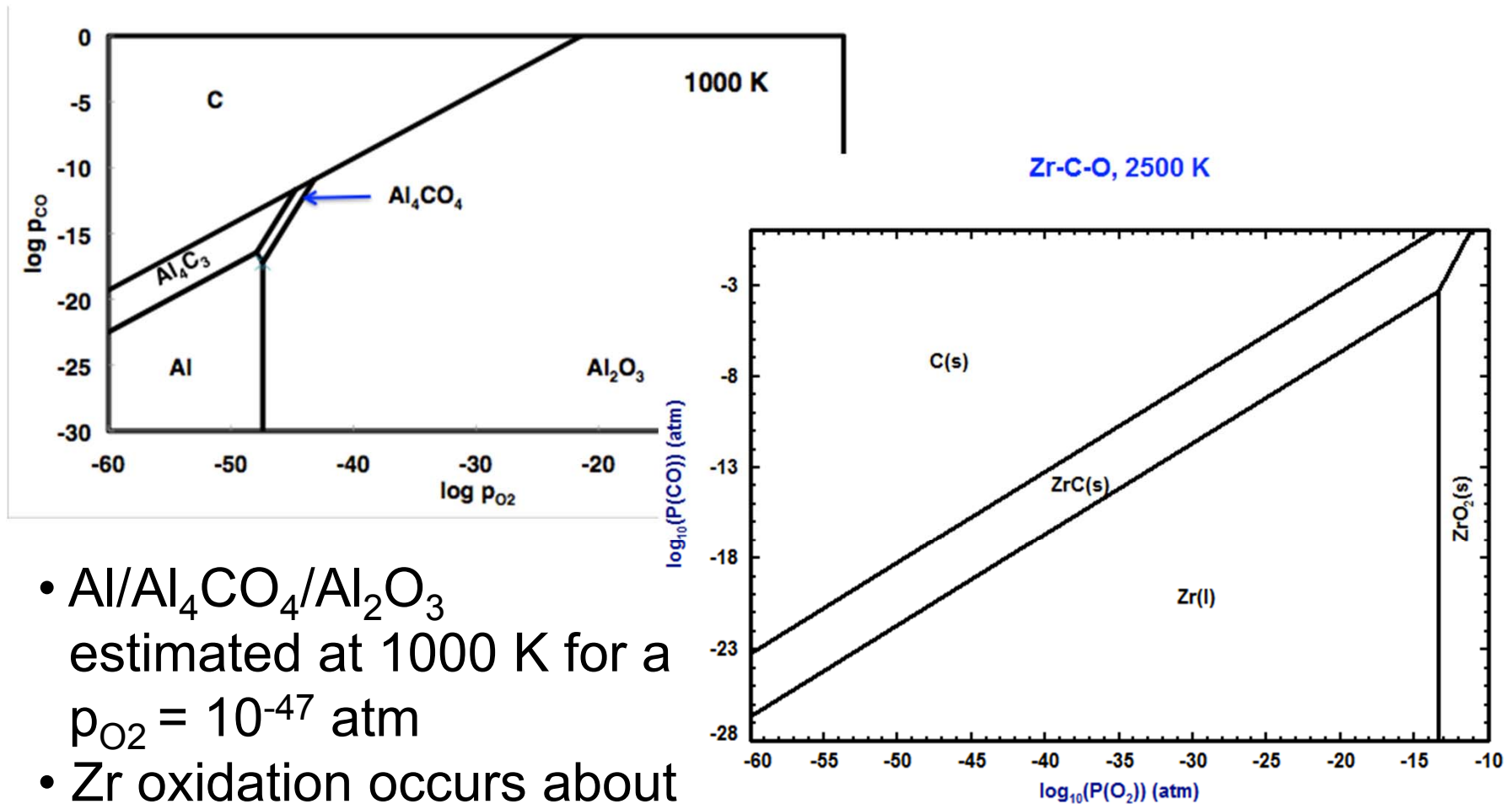


## Configuration of Ti-Al-C reaction system

- Ti-Al-C charged to graphite crucibles heated to 1600-1700° C.
- Closed thermodynamic system controls oxygen potential.
- Al/Al<sub>4</sub>CO<sub>4</sub>/Al<sub>2</sub>O<sub>3</sub> establishes  $p_{O_2}$  at 1000 K (follows concept of Komarek research group using pseudo-isopiestic technique).

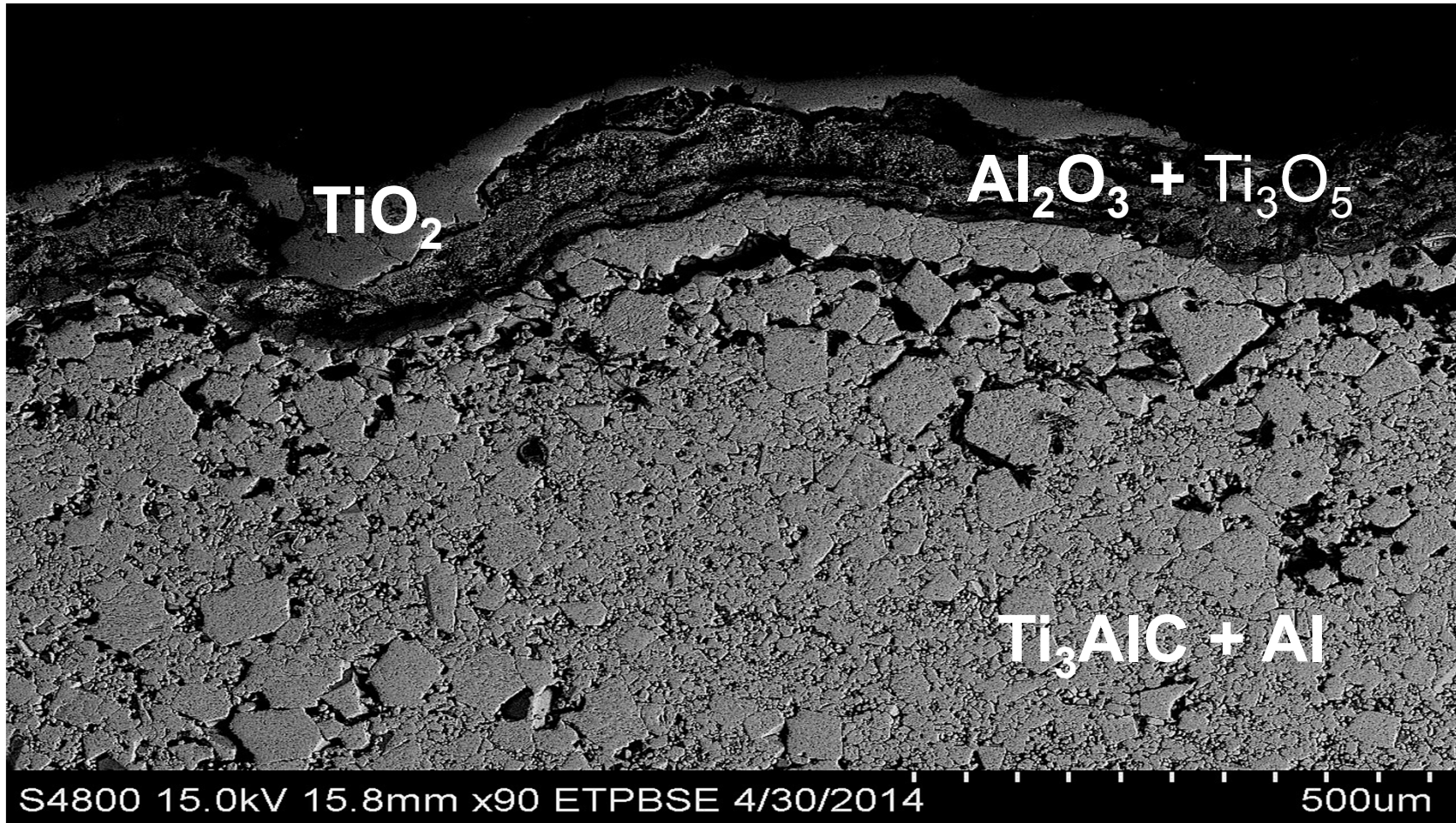


## Stability of Al-C-O System at 1000 K and Zr-C-O System at 2500 K



- Al/ $Al_4CO_4$ / $Al_2O_3$  estimated at 1000 K for a  $p_{O_2} = 10^{-47}$  atm
- Zr oxidation occurs about  $10^{-13}$  atm.

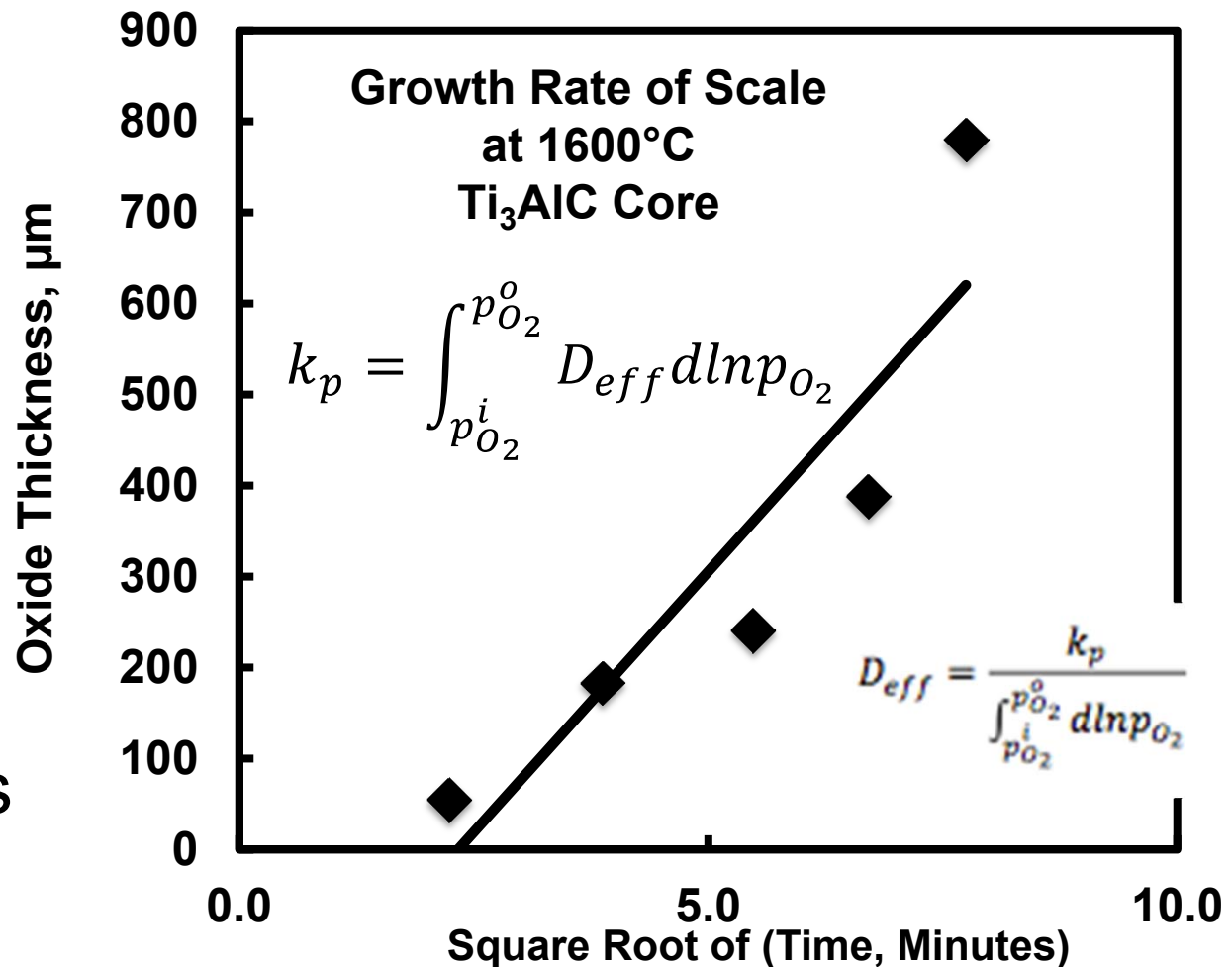
***Ti<sub>3</sub>AlC core after 30 minute oxidation at 1600° C***



# Parabolic Growth Rate of Scale

□  $D_{\text{eff}} = 6.2 \times 10^{-8} \text{ cm}^2/\text{s}$   
 from slope via measured scale.

□ For  $\text{Al}_2\text{O}_3$  scale at 1873 K,  $D_{\text{eff}} = 2.6 \times 10^{-13} \text{ cm}^2/\text{s}$   
 Calculated from Equation of Ramanarayanan et al. -- 1984





## Extending Previous Kinetic Equations

- Grabke's equations [1965 and 1970] for oxygen transfer on metals (e.g., Fe)

$$\frac{dn_o}{dt} = ka_o^{-m} p_{CO_2} - ka_o^{1-m} p_{CO}$$
- Wang et al. [2003] determined oxidizing sequence for Ti44Al11Nb alloy with X-ray photoelectron spectroscopy.

$$O_2 + 2V = 2O_{ad}$$

$$Al + O_{ad} \rightarrow AlO$$

$$AlO + O_{ad} \rightarrow AlO_2$$

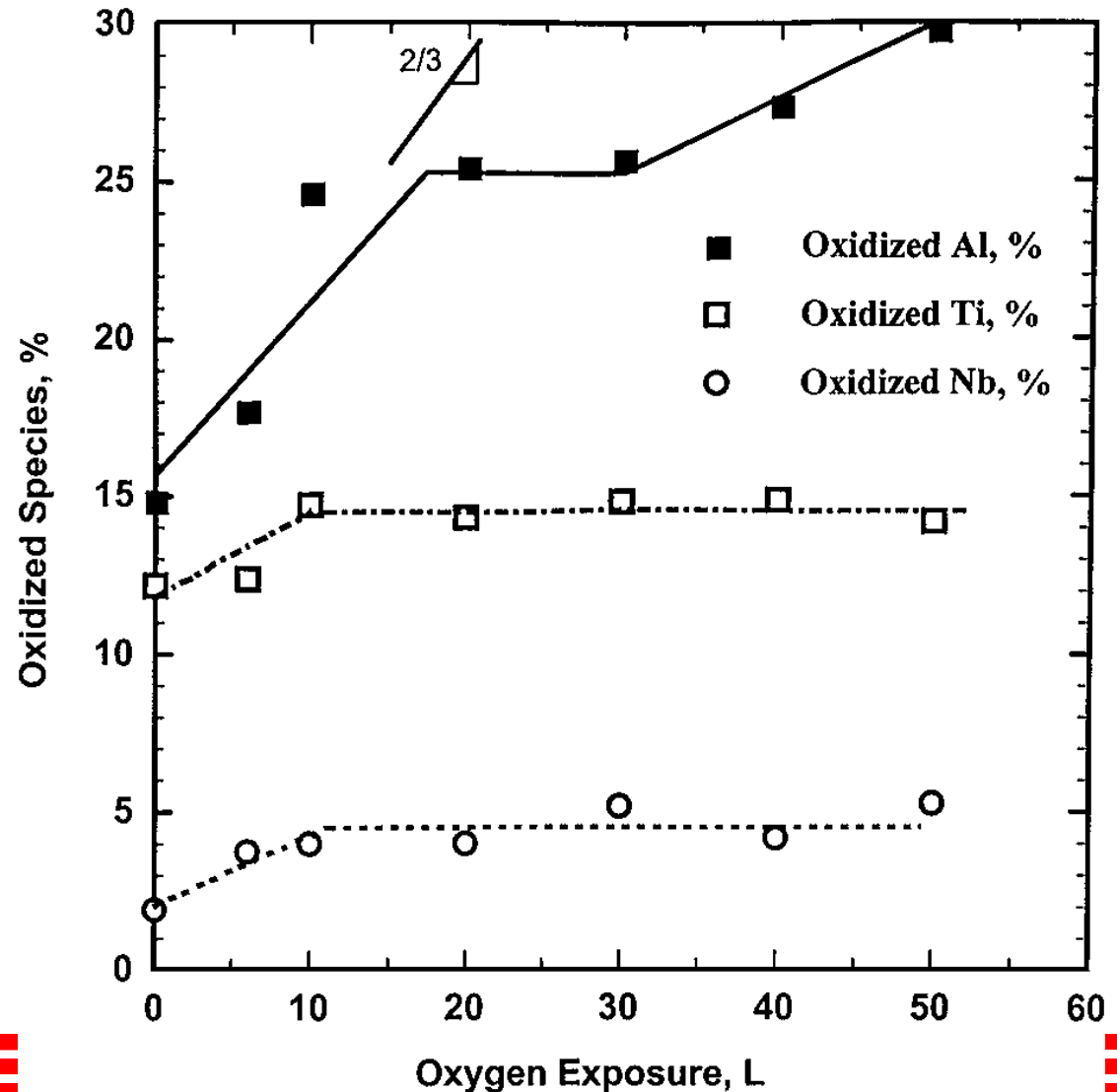
$$AlO_2 + O_{ad} \rightarrow AlO_3$$
- Kurunczi, Guha and Donnelly [2006] on adsorption of oxygen ( $O_{ads}$ ) on surface sites (V) from O<sub>2</sub> plasma

$$Og + V \rightarrow O_{ads}$$

$$2O_{ads} \rightarrow O_{2(g)} + 2V$$

# **Oxidized Species Measured on Ti-44Al-11Nb (at%) with X-ray Photoelectron Spectroscopy**

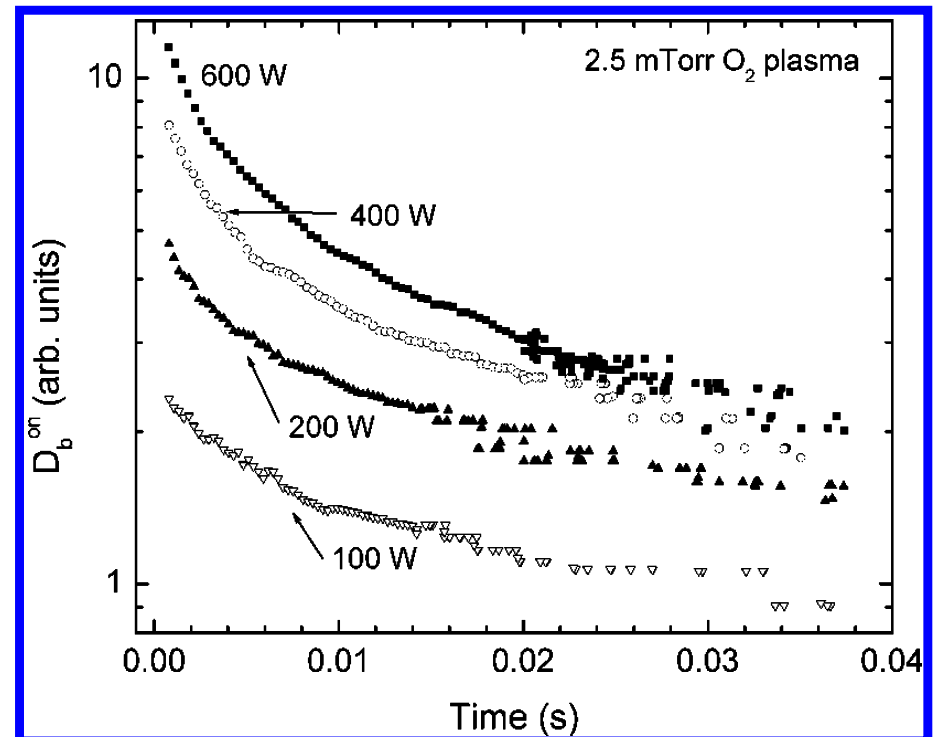
- Oxygen exposure of  $L = t \cdot p_{O_2}$  ( $10^{-6}$  Torr·s)
- Slope of 2/3 acquired from kinetic rates of oxygen adsorption per  $AlO_3$  formation ( $r_{ad}/r_{AlO_3}$ )



# Merge the kinetics of oxygen adsorption to experimental plasma data

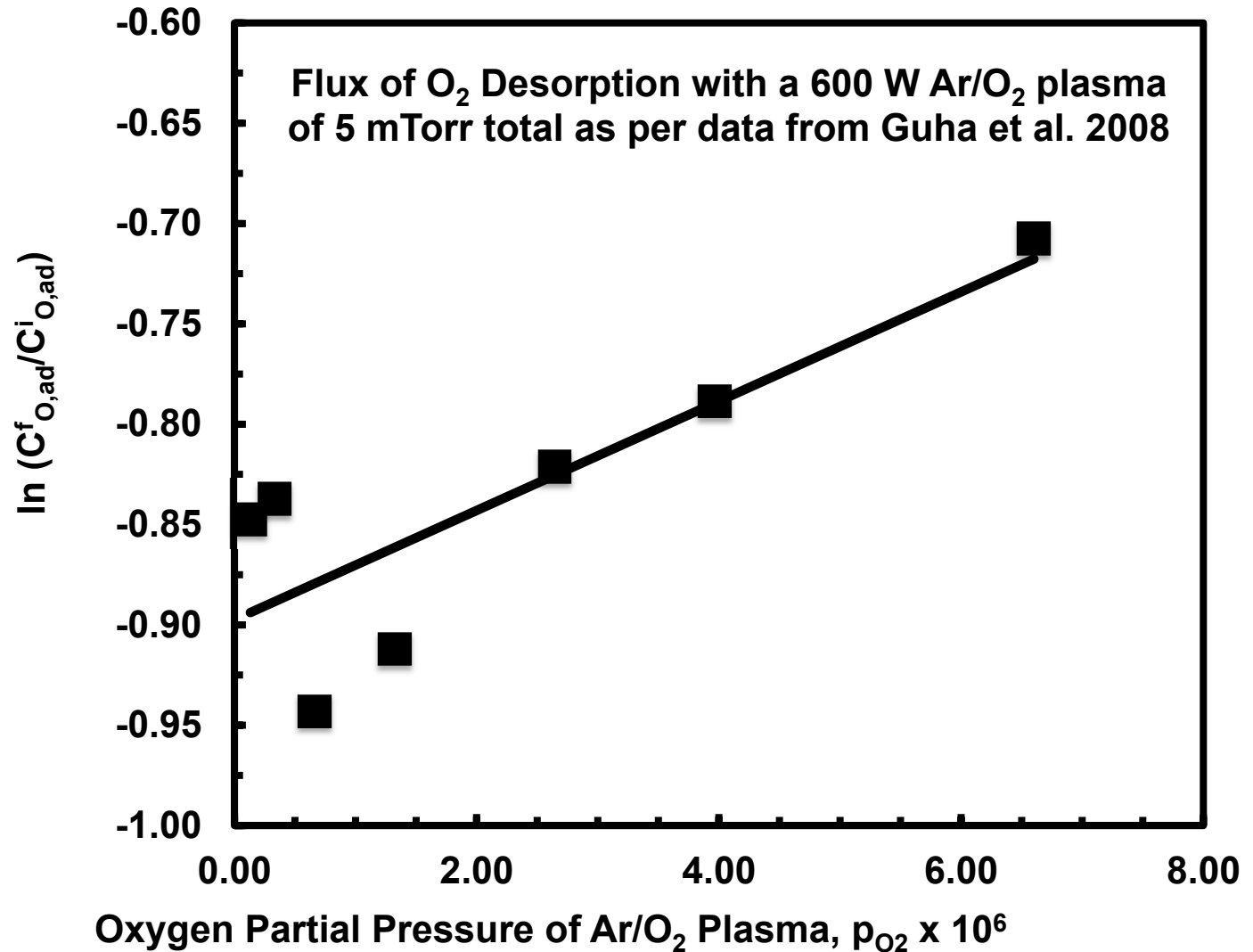
- Apply the reaction scheme by Wang et al. (2003) to experimental plasma data by Kurunczi, Guha and Donnelly (2006).
- Determine the effect of plasma via the ionizing power on  $C_{\text{AlO}_3}$ .

$$\ln \left[ \frac{C_{\text{O},ad}^f}{C_{\text{O},ad}^i} \right] = S\alpha t$$





## Interpretation of Desorbed Ar/O<sub>2</sub> Plasma



# **Summary**

- Used COMSOL, a commercial software package, to obtain the temperature profile of a packed bed of  $B_4C$ .
- Analyzed **thermodynamic stability of oxygen potentials for  $TiO_x$**  and  $TiO_x-Al_2O_3$  for possible scale formation from  $Ti_2AlC$ - $TiC$  components.
- **Controlled oxygen potential** to form  $Ti_3AlC$ -Al composite which follows parabolic oxidation.
- Examined **the plasma-surface reactions** on Al oxide surface.
- Determining the effect of **charged surface sites attracting ultimately the oxygen** for surface reactions.





# *Questions and Comments*



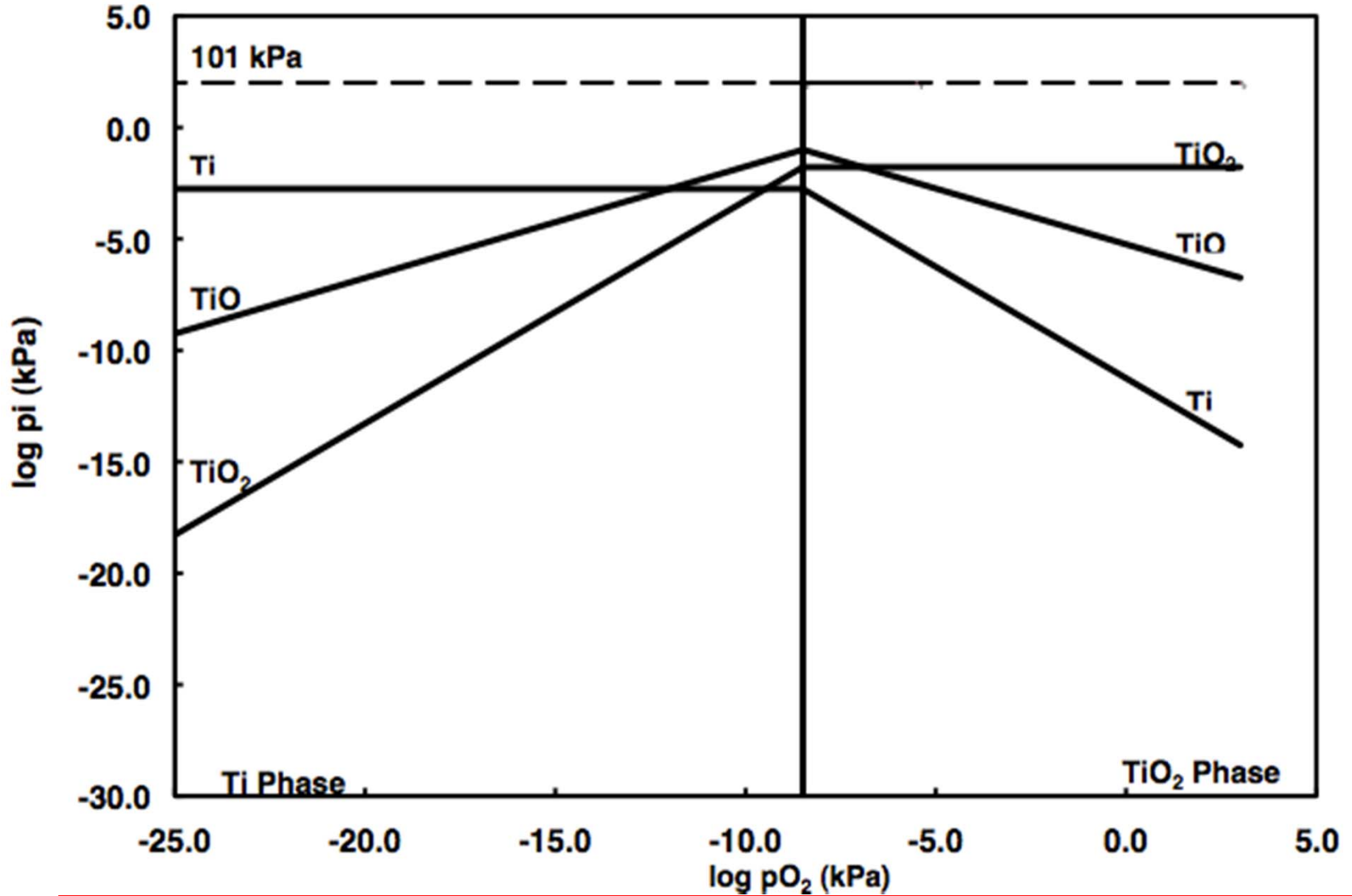


***Slides to Respond to  
Possible Queries Follow***





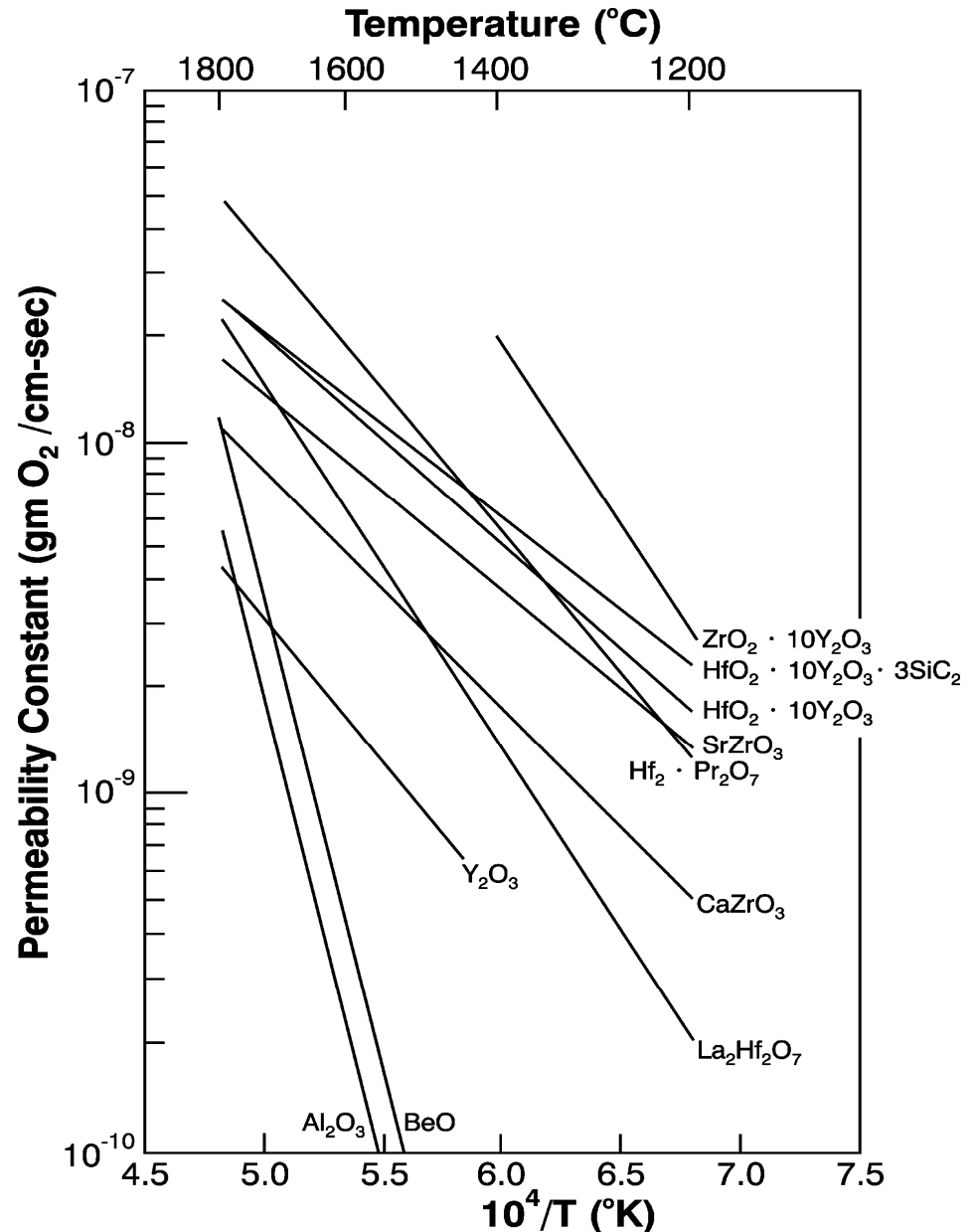
# Kellogg Diagram for Ti-O System (2500 K)





# Oxygen Permeability

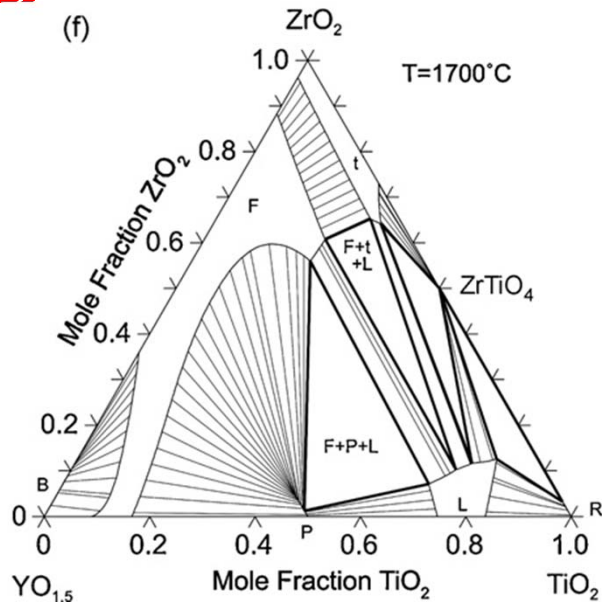
- For temperatures between 1700 to 1500° C  $\text{Al}_2\text{O}_3$  and  $\text{Y}_2\text{O}_3$  have oxygen permeability  $\leq 10^{-9}$   $\text{gO}_2/(\text{cm}\cdot\text{s})$  and  $3\cdot 10^{-9}$   $\text{gO}_2/(\text{cm}\cdot\text{s})$ , respectively.
- Oxygen permeability of  $\text{ZrO}_2\text{-Y}_2\text{O}_3$  and  $\text{HfO}_2\text{-Y}_2\text{O}_3$  increases by approximately an order of magnitude [i.e.,  $\geq (10)^{-8}$   $\text{gO}_2/(\text{cm}\cdot\text{s})$ ].



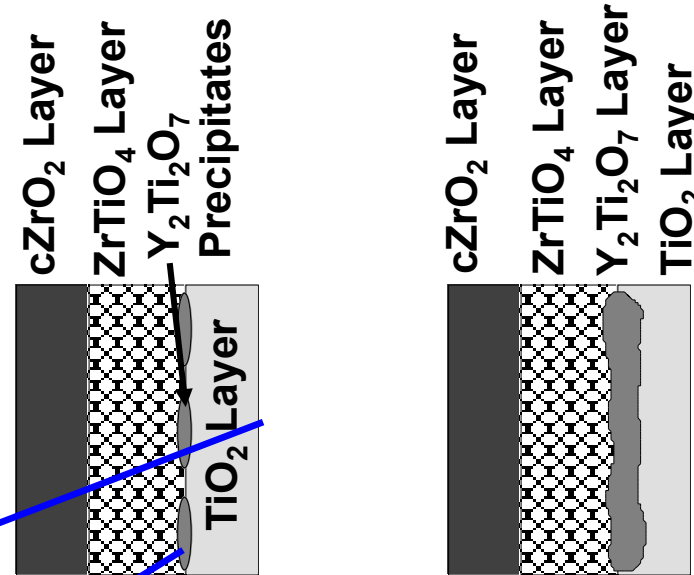
(Opeka, Talmy & Zaykoski-2004)



# Wagner's Rate Equation for Scales



Calculated Diagram from Schaedler,  
Fabrichnaya and Levi -- 2008

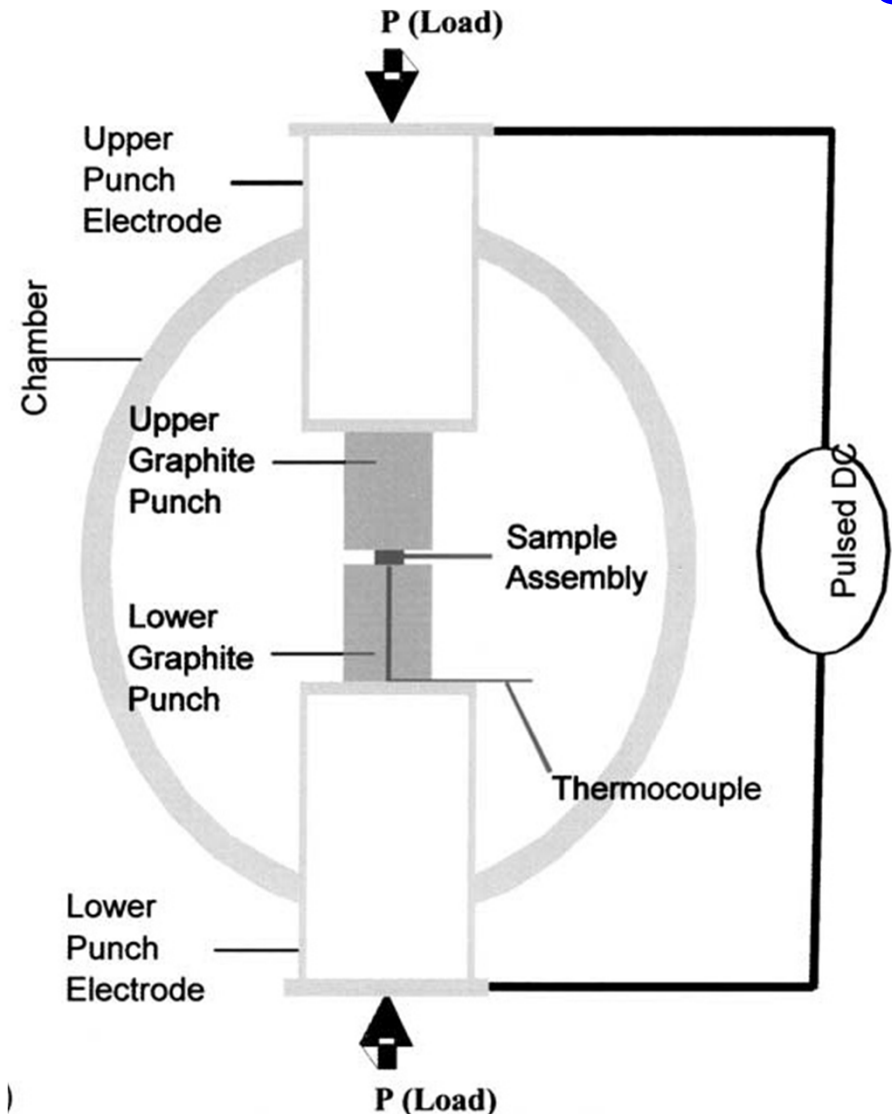


$$\frac{1}{A} \frac{d\tilde{n}}{dt} = \frac{1}{\xi} \left[ \frac{\tilde{c}}{2} \int_{p_{O_2}^{(i)}}^{p_{O_2}^{(o)}} \left( \left( \frac{z_M}{z_O} \right) D_M + D_O \right) d \ln p_{O_2} \right] = \frac{\tilde{k}}{\xi}$$



# Thoughts on Spark-Plasma Sintering

- Plasma has been professed to enhance sintering but **without ionized gas evidence**.
- Current pulses passes through graphite – sample though **configuration affects the temperature extremes developed**.
- **What percentage of electromigration and thermal diffusion contributes to sintering?**



## ***Future Efforts for Plasma Surface Reactions***

- **Incorporate electron energy** (e.g., electron energy density ( $n_\varepsilon$ ), gradient of electron flux vector ( $\Gamma_\varepsilon$ ) and potential field ( $\mathbf{E}$ )).

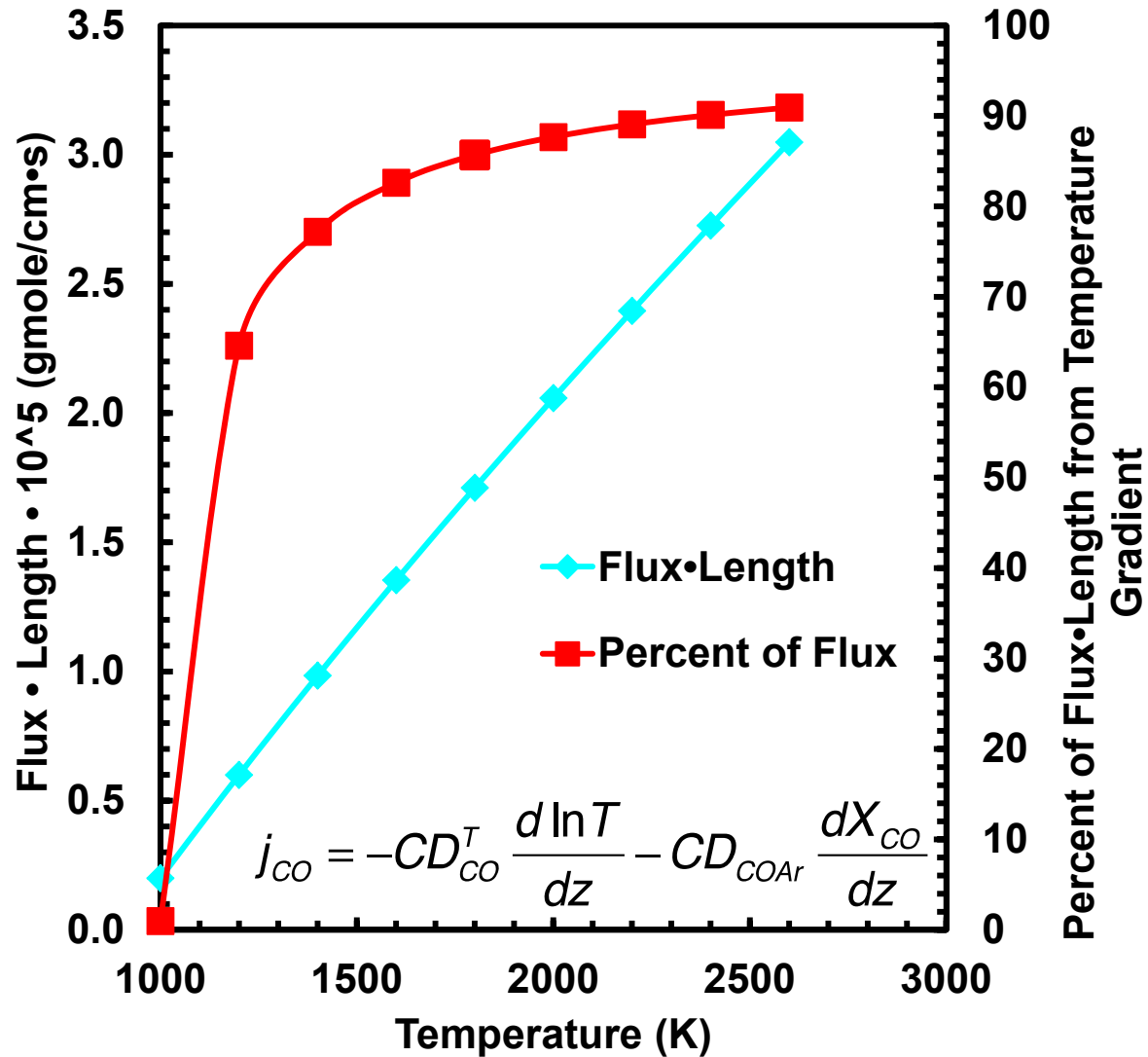
$$\frac{\partial}{\partial t}(n_\varepsilon) + \nabla \cdot \Gamma_\varepsilon + \mathbf{E} \cdot \Gamma_\varepsilon = R_\varepsilon - (\mathbf{u} \cdot \nabla)n_\varepsilon$$

- **Incorporate kinetics of Ar-O<sub>2</sub> plasma-surface reactions** with SiC and Ti<sub>2</sub>AlC.
- **Study the effect of temperature extremes** (T and dT/dx) on **metastable phases and/or segregation**.





# Diffusional Flux – Kinetics Issues



□  $D_{COAr}$  from Poirier-Geiger and checked with Chapman-Enskog Eq.

□ Mean temperature

$$\frac{T_H T_C}{T_H - T_C} \ln \frac{T_H}{T_C} = 1527K$$

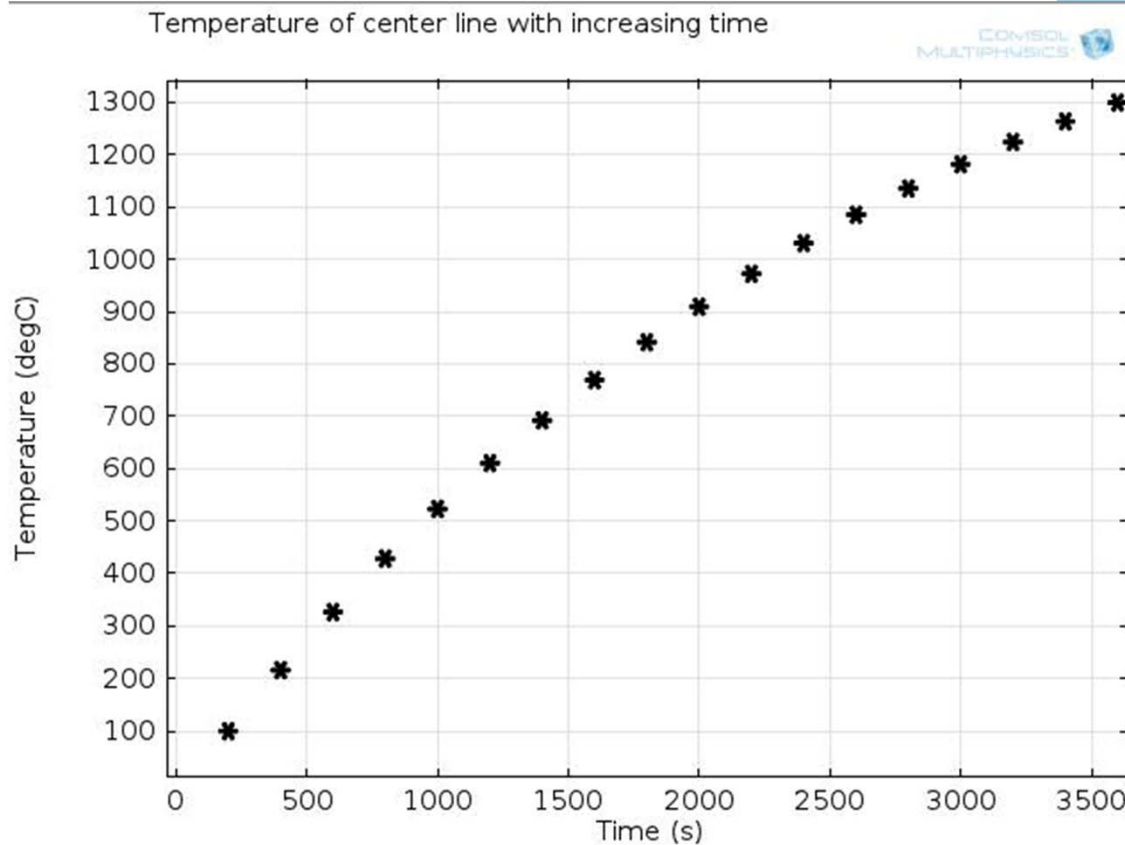
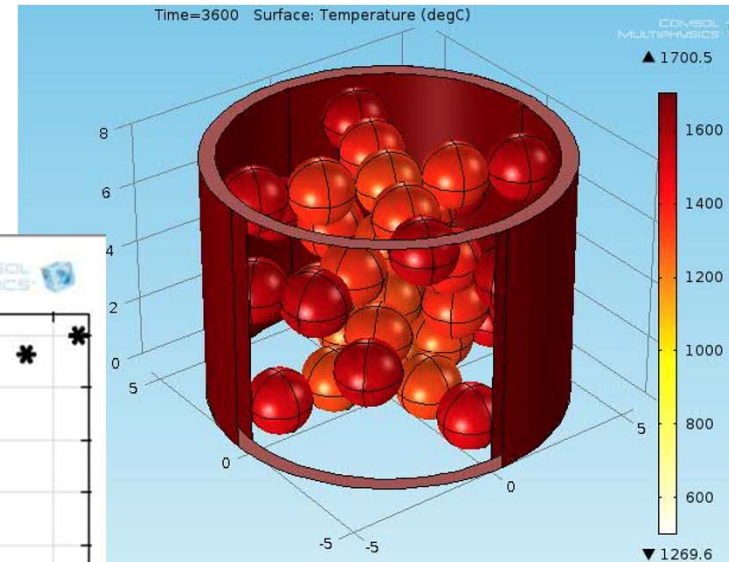
□ Al/Al<sub>2</sub>O<sub>3</sub>/Al<sub>4</sub>CO<sub>4</sub> reaction rate?





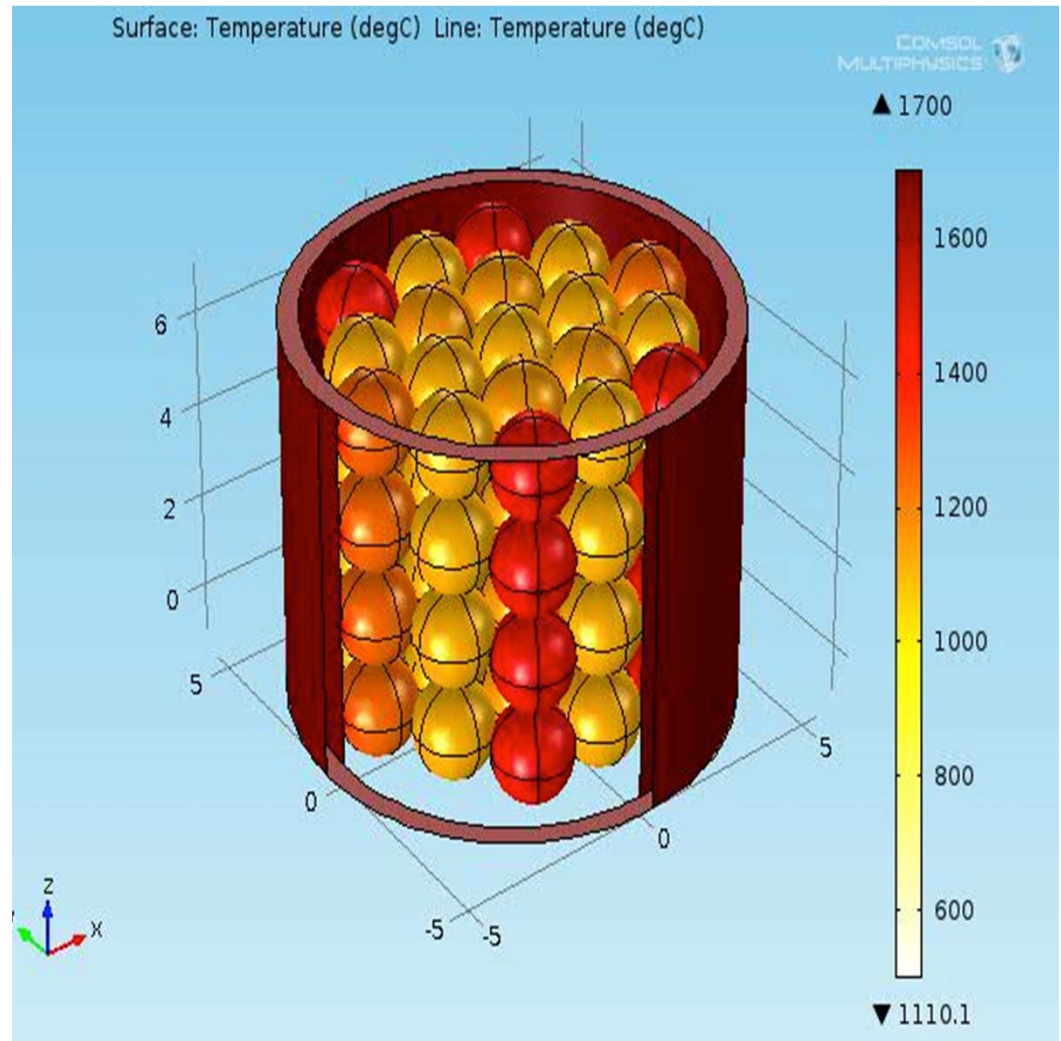
# COMSOL Simulation of $B_4C$ Spheres Basis for Packed Bed with Temperature Profile

- Carbide spheres configured in an X-pattern rotating along centerline.
- The spheres have an open structure.



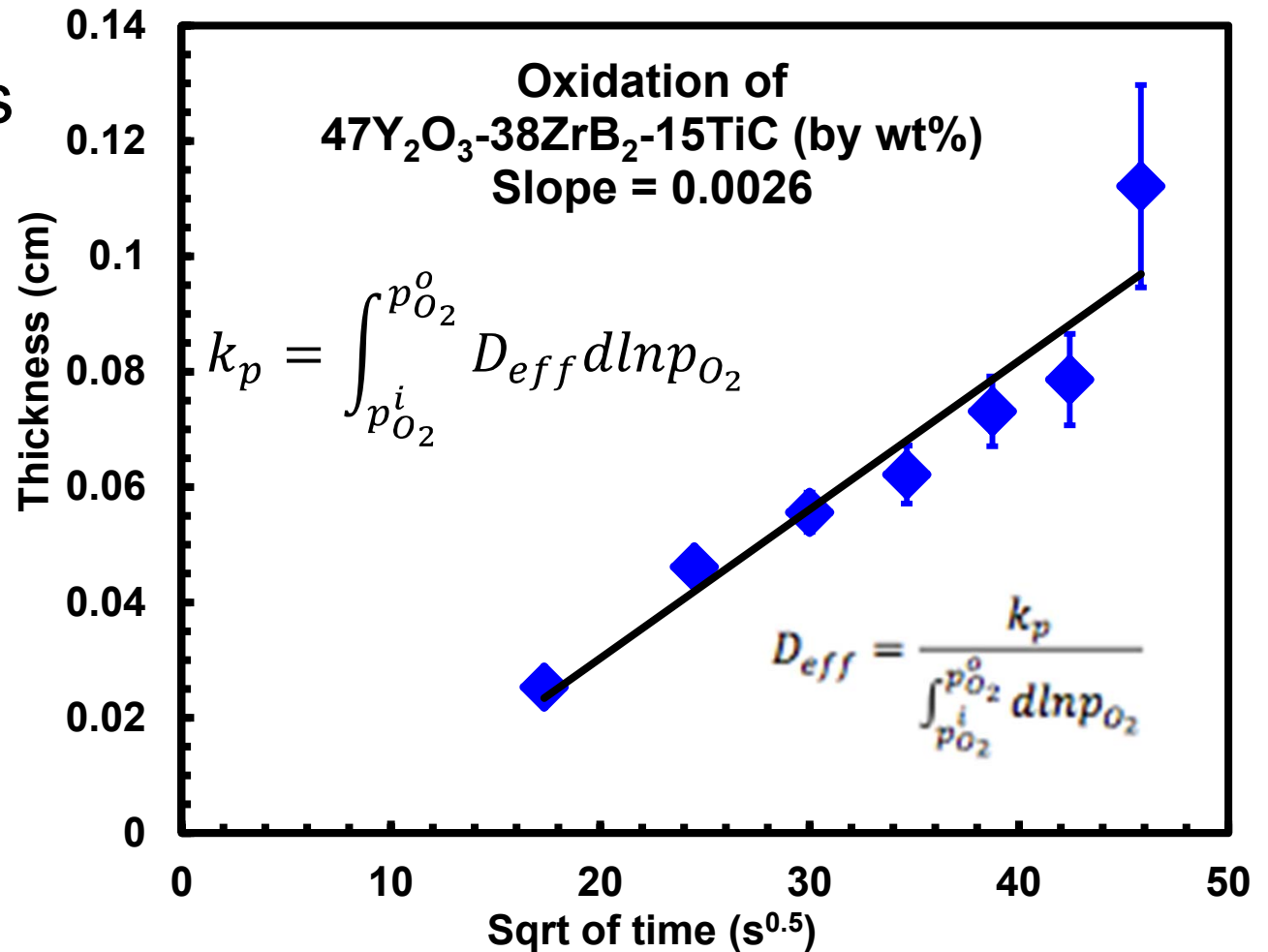
# COMSOL Simulation of $B_4C$ spheres in a packed bed

- Cylindrical graphite wall temperature is heated mimicking internal furnace wall.
- Carbide spheres touch each other with a 6-fold lateral configuration though each layer contacts uniformly.
- Spheres contacting the wall have highest temperature.
- Conductive heat transfer was used, but radiation will be added with expanded sphere number.



# Parabolic Growth Rate of Scale

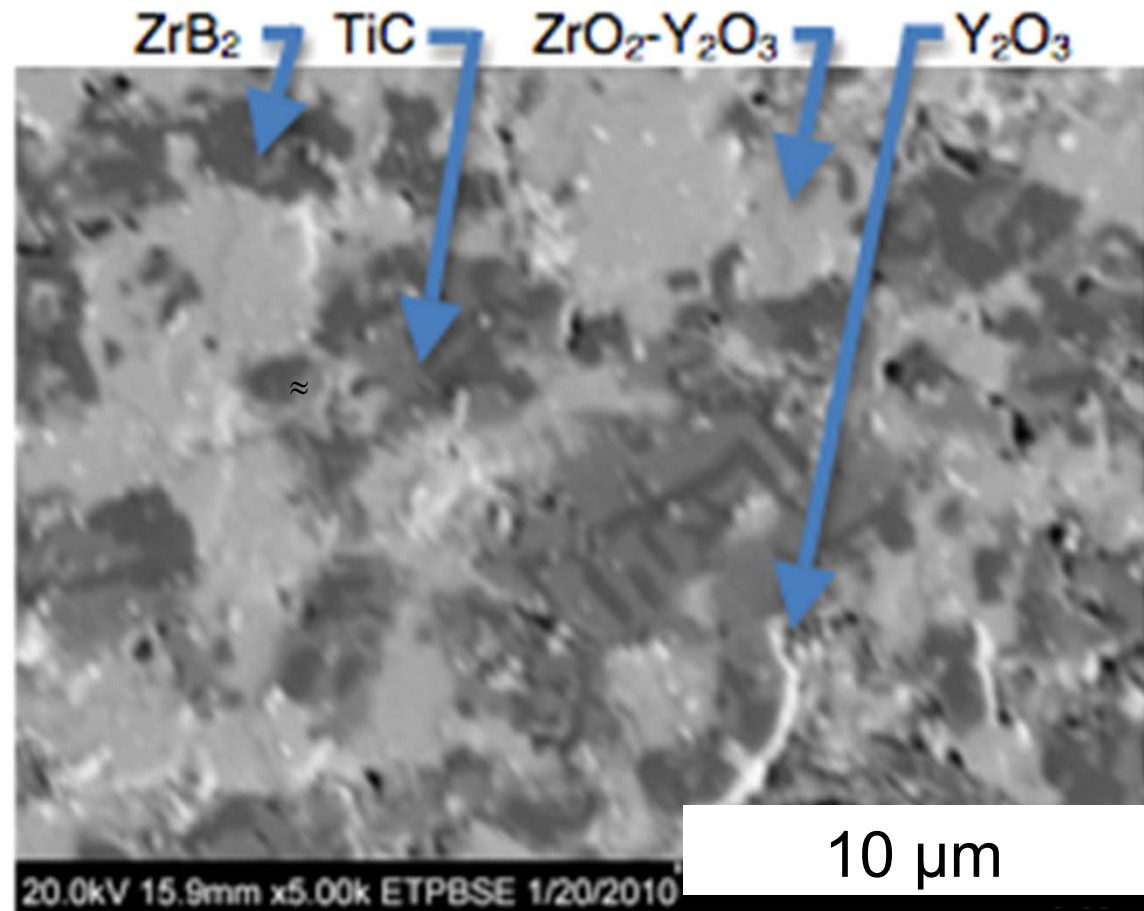
□  $D_{\text{eff}} = 10^{-11} \text{m}^2/\text{s}$   
for t-ZrO<sub>2</sub>-Y<sub>2</sub>O<sub>3</sub>  
phase as  
controlling layer





## **SEM image after spark-plasma sintering (SPS)\* of $ZrB_2$ -TiC- $Y_2O_3$**

- $ZrB_2$  oxidizes to  $ZrO_2$  dissolving some  $Y_2O_3$ .
- Stringers of  $Y_2O_3$  appear in grain boundary.
- Graphite minimized TiC oxidation though TiO formed from residual  $O_2$  in Ar.



\* SPS done at Dr. Erica Corral's Laboratory at U of Arizona

# *Electron-Energy Transport*

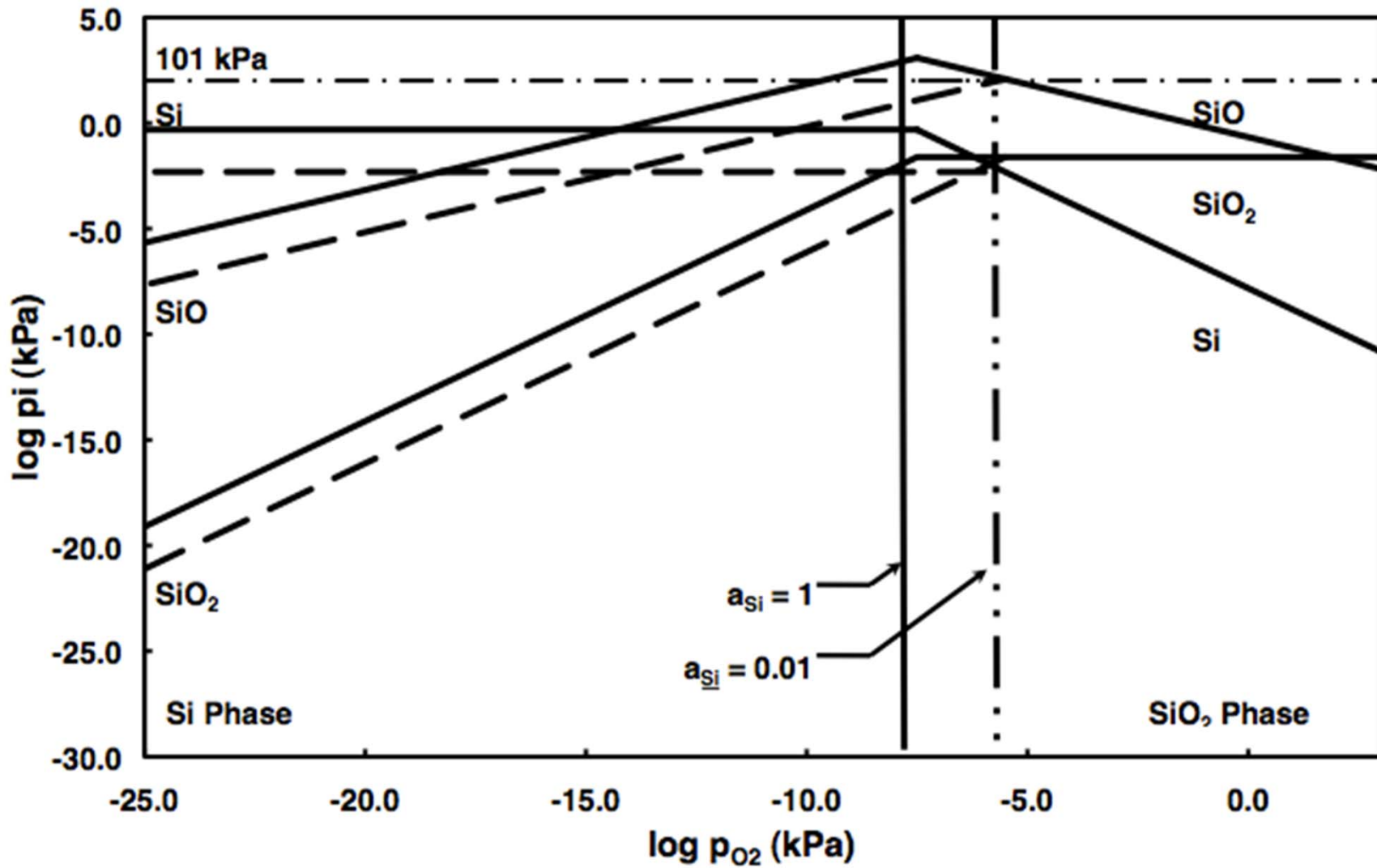
- Should consider electron, ions and neutral species balance coupled with electron energy and momentum balances.

$$\frac{\partial}{\partial t} (n_{\varepsilon}) + \nabla \cdot \Gamma_{\varepsilon} + \mathbf{E} \cdot \Gamma_{\varepsilon} = R_{\varepsilon} - (\mathbf{u} \cdot \nabla) n_{\varepsilon}$$

$$\frac{\partial}{\partial t} (n_e) + \nabla \cdot [-n_e(\mu_e \cdot \mathbf{E}) - \mathbf{D}_e \cdot \nabla n_e] = R_e$$

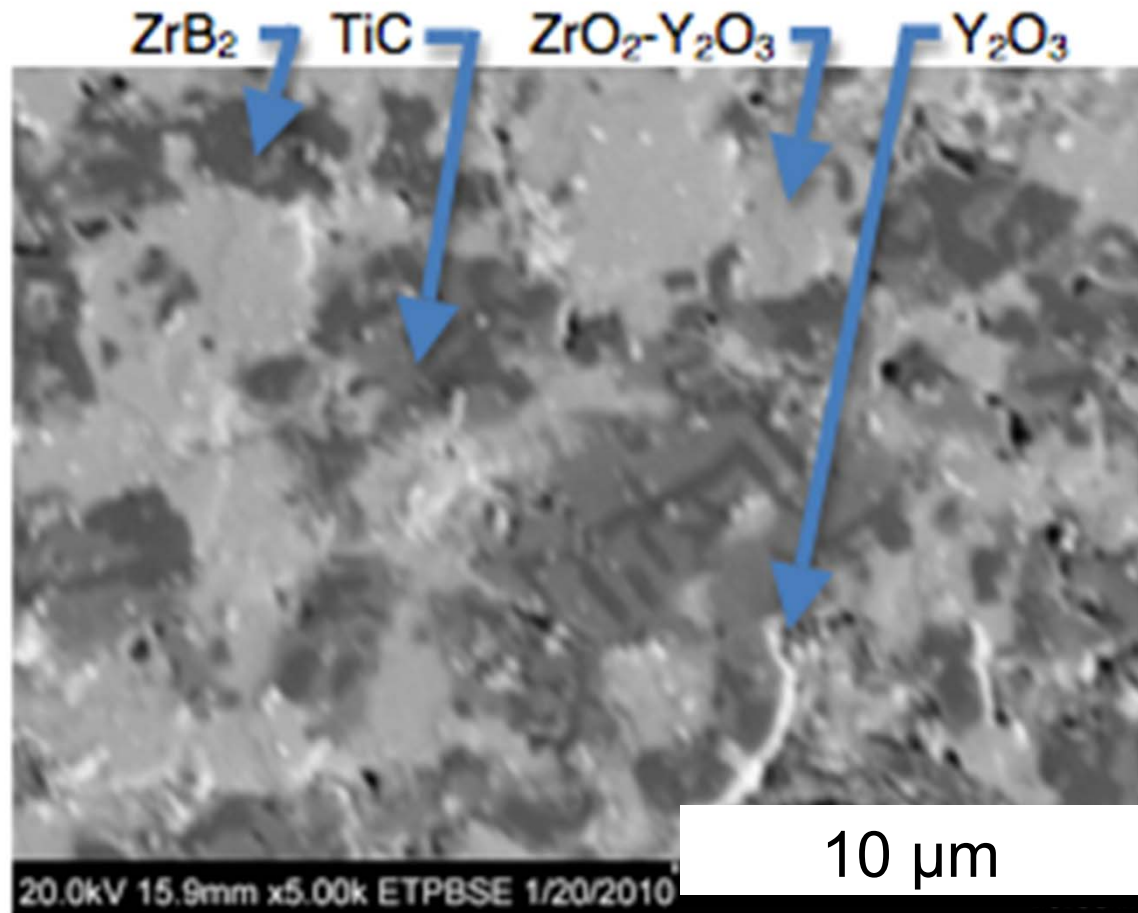


# Kellogg Diagram for Si-O System (2500 K)



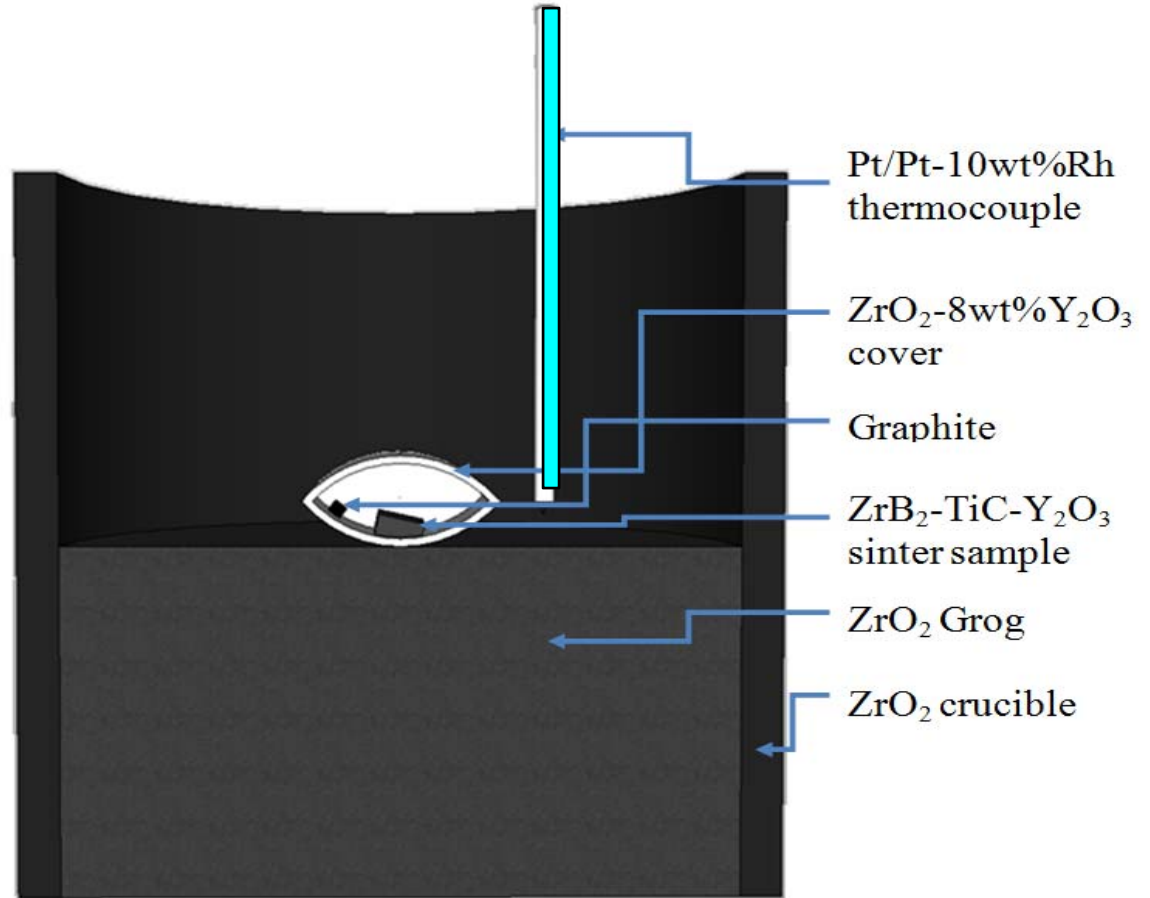
## **SEM image after spark-plasma sintering**

- $\text{ZrB}_2$  oxidizes to  $\text{ZrO}_2$  dissolving some  $\text{Y}_2\text{O}_3$
- Stringers of  $\text{Y}_2\text{O}_3$  appear in grain boundary
- Graphite seems to minimize TiC oxidation.



# **Oxidation in Silicide Furnace with air and C/CO/N<sub>2</sub> atmospheres at 1700° C**

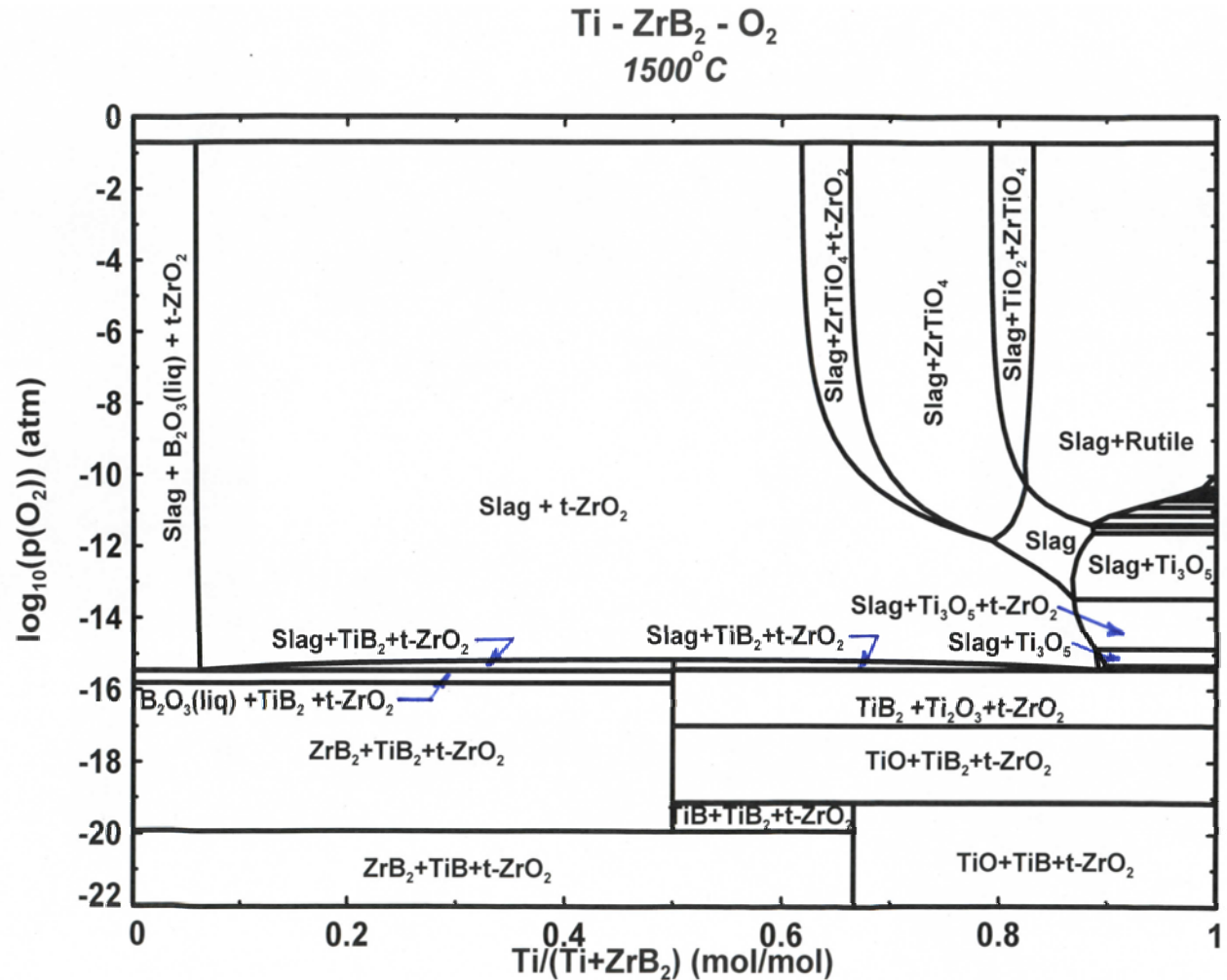
- Spark plasma-sintered samples
- ZrO<sub>2</sub>-8 wt% Y<sub>2</sub>O<sub>3</sub> crucible covers were used to hold samples.
- Hf foil were also used to hold samples.





# Oxygen Levels for $TiO_x$ with Calculated $Ti-ZrB_2-O_2$ Phase Diagram

- Ti oxides start to form near  $p_{O_2} > 10^{-22}$  atm with TiO.
- $Ti_2O_3/Ti_3O_5$  has  $p_{O_2} = 10^{-15.5}$  atm
- $ZrB_2$  oxidizes to  $t-ZrO_2$  with Ti oxides.
- Liquid oxides form with increasing  $p_{O_2}$

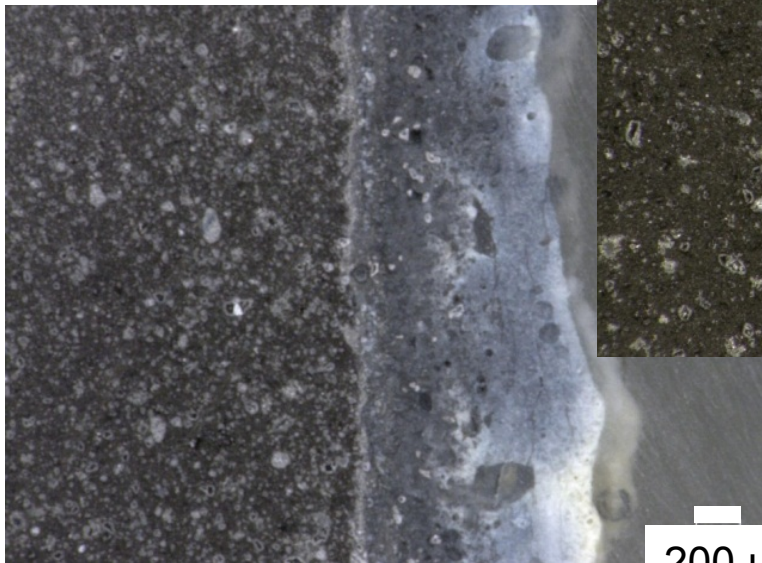




# *Optical Microstructures to Measure Scale*

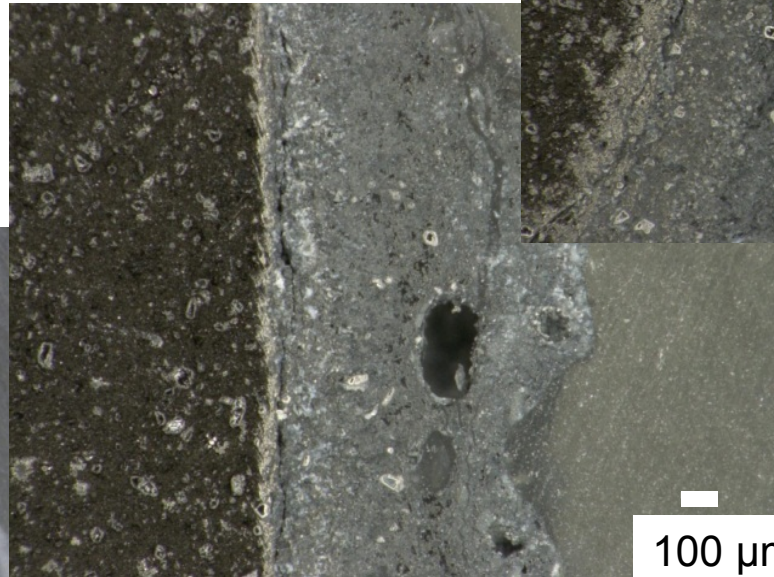
Increasing Oxidizing Time

20 minutes



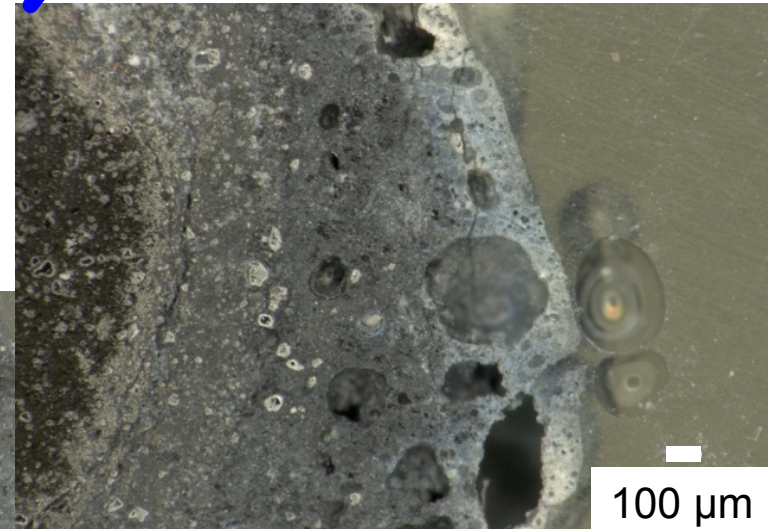
200  $\mu\text{m}$

30 minutes



100  $\mu\text{m}$

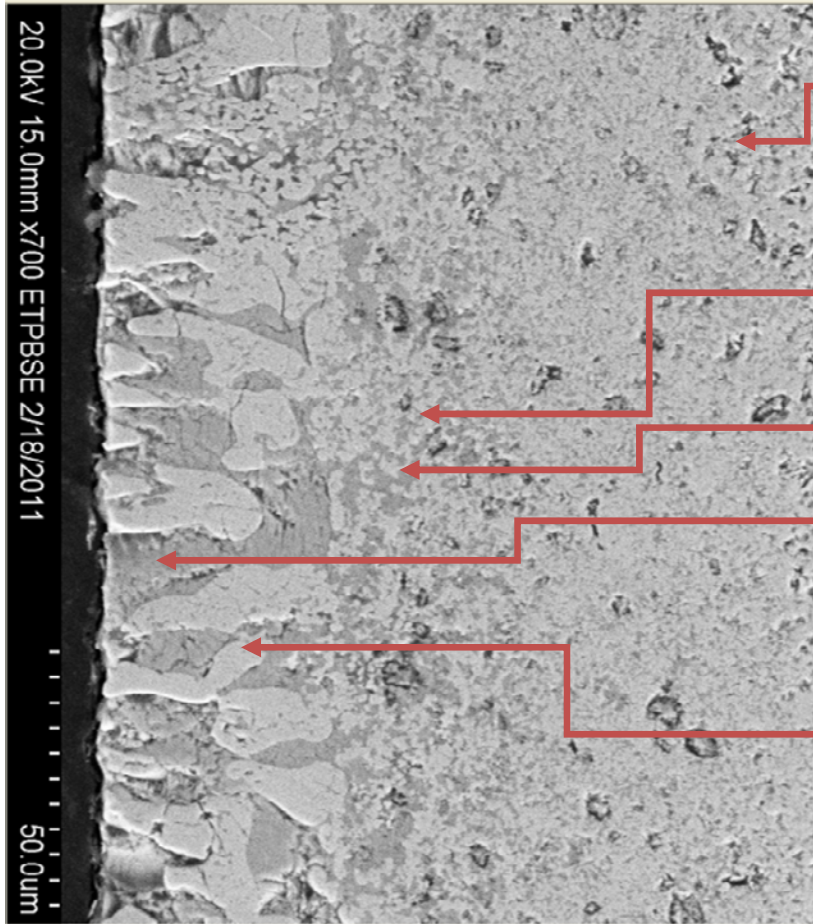
35 minutes



100  $\mu\text{m}$



# Phases identified for oxidized sample in C/CO/N<sub>2</sub>



ZrB<sub>2</sub>-TiC-  
Y<sub>2</sub>O<sub>3</sub>

Y<sub>2</sub>O<sub>3</sub>

ZrO<sub>2</sub>-TiO<sub>2</sub>-Y<sub>2</sub>O<sub>3</sub>

Y<sub>2</sub>O<sub>3</sub>

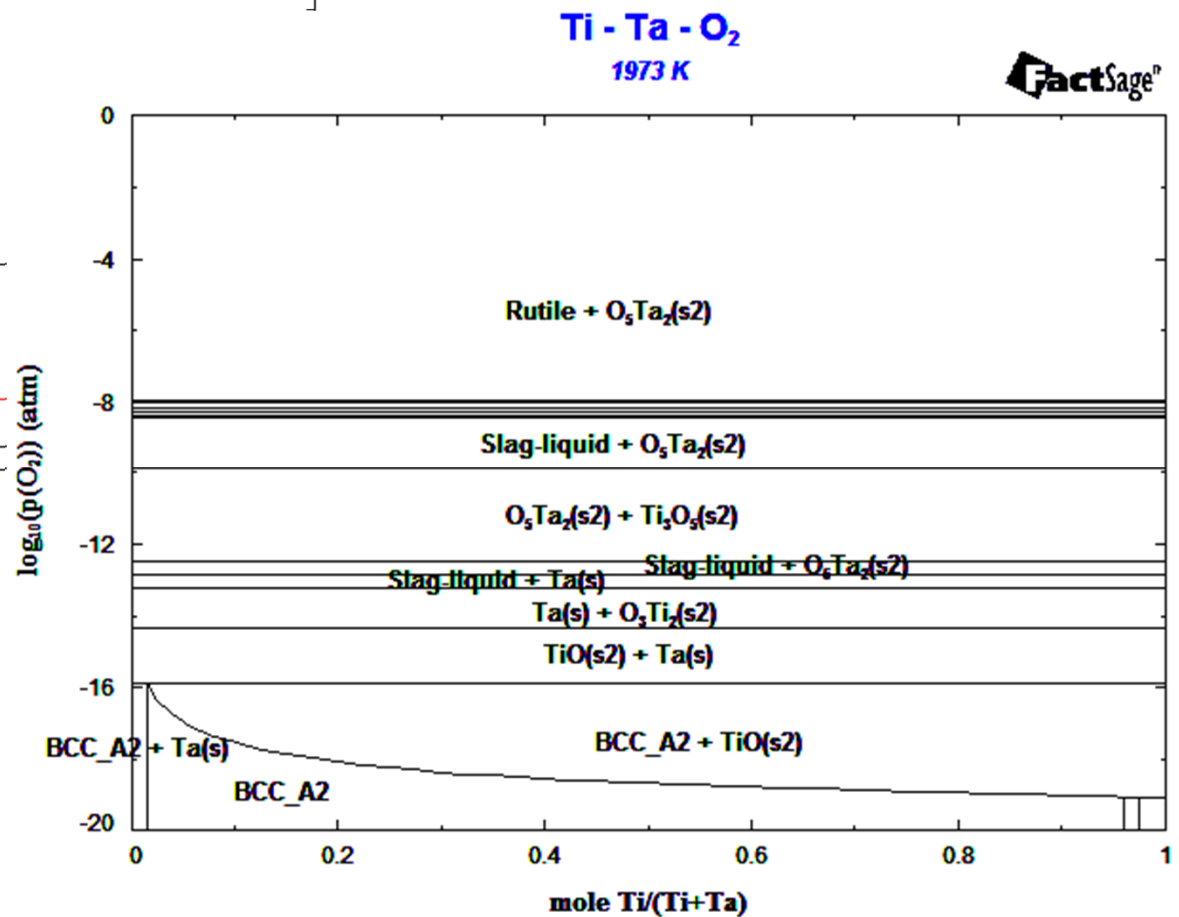
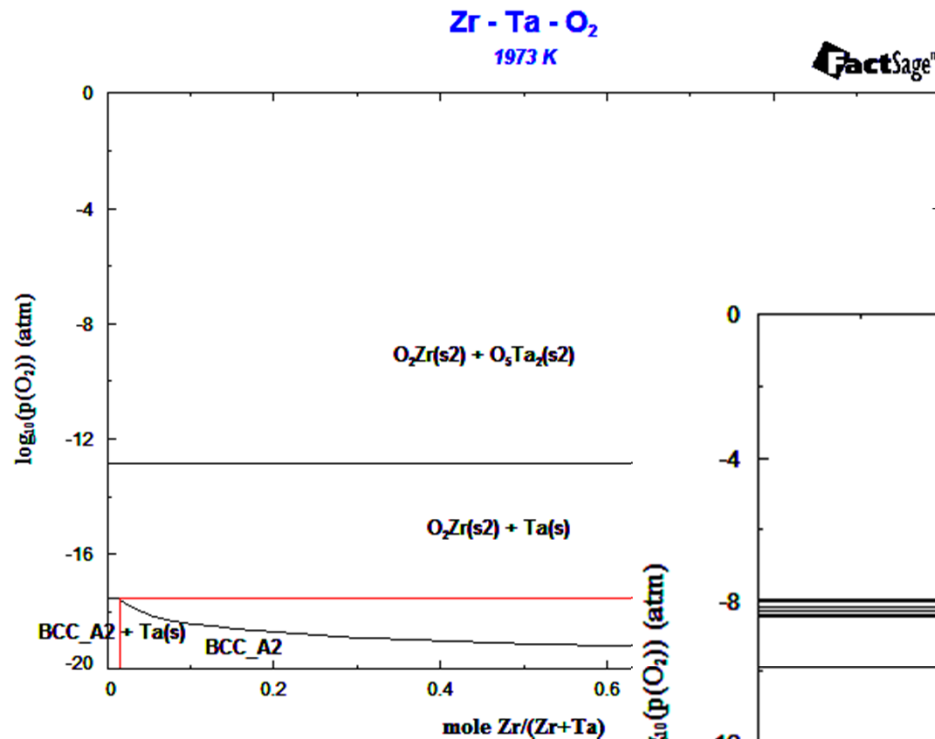
ZrO<sub>2</sub>







# Calculated Zr-Ta-O<sub>2</sub> and Ti-Ta-O<sub>2</sub> phase diagrams

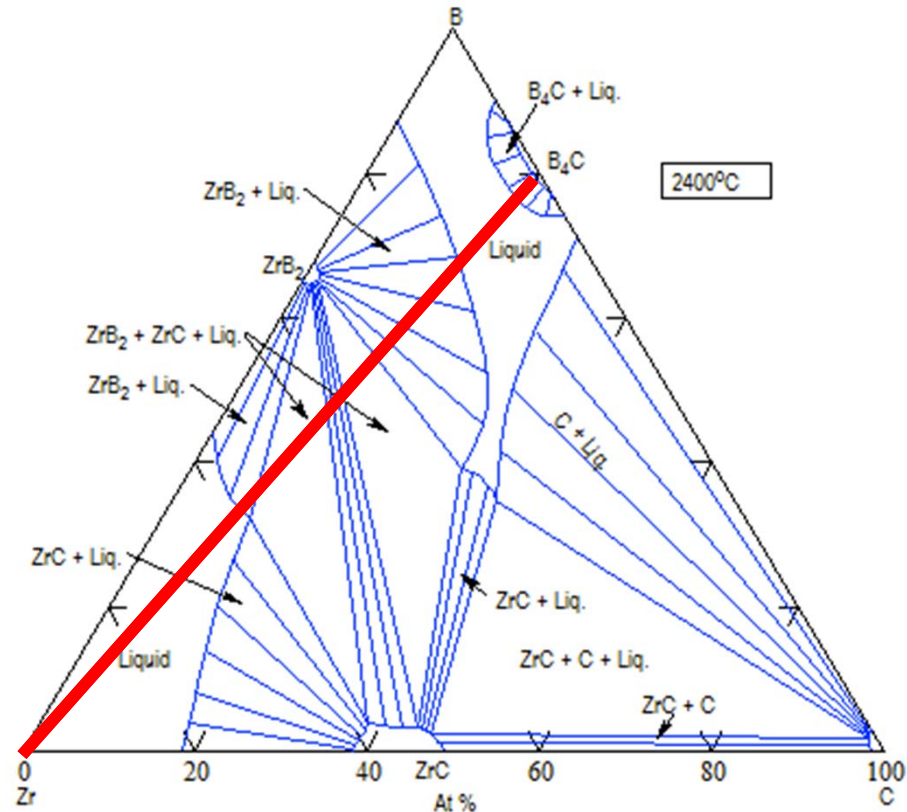


- p<sub>O2</sub> level for Ta/Ta<sub>2</sub>O<sub>5</sub>
- TiO<sub>x</sub>-Ta<sub>2</sub>O<sub>5</sub> liquids

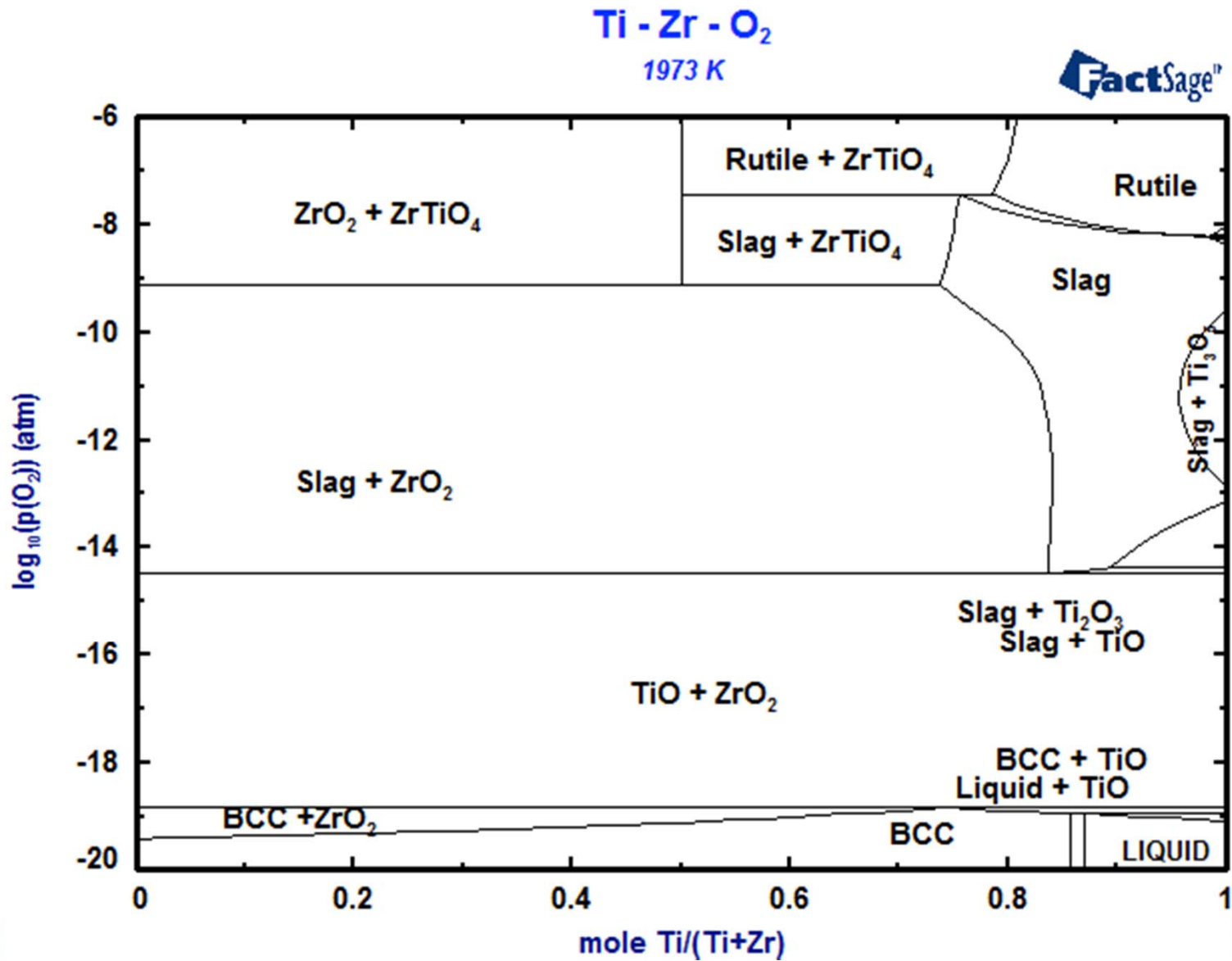


# **Zr as primary component in $B_4C$ reaction on Zr-B-C phase diagram**

- Zr liquid changes with alloy composition
- Zr reacts with  $B_4C$  forming ZrC and  $ZrB_2$  as a result of the mass balance.

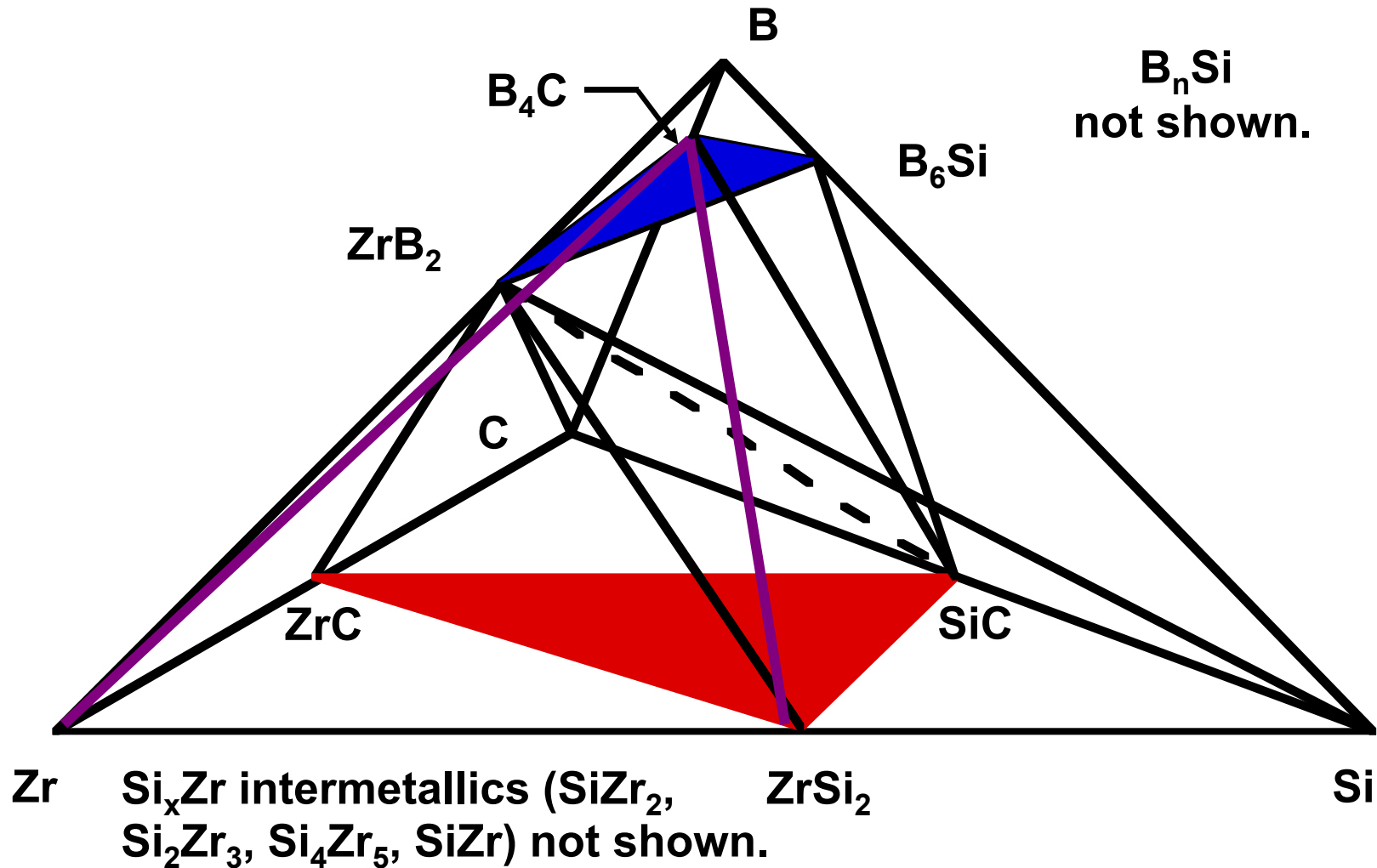


# Ti-Zr-O<sub>2</sub> Phase Diagram at 1973 K



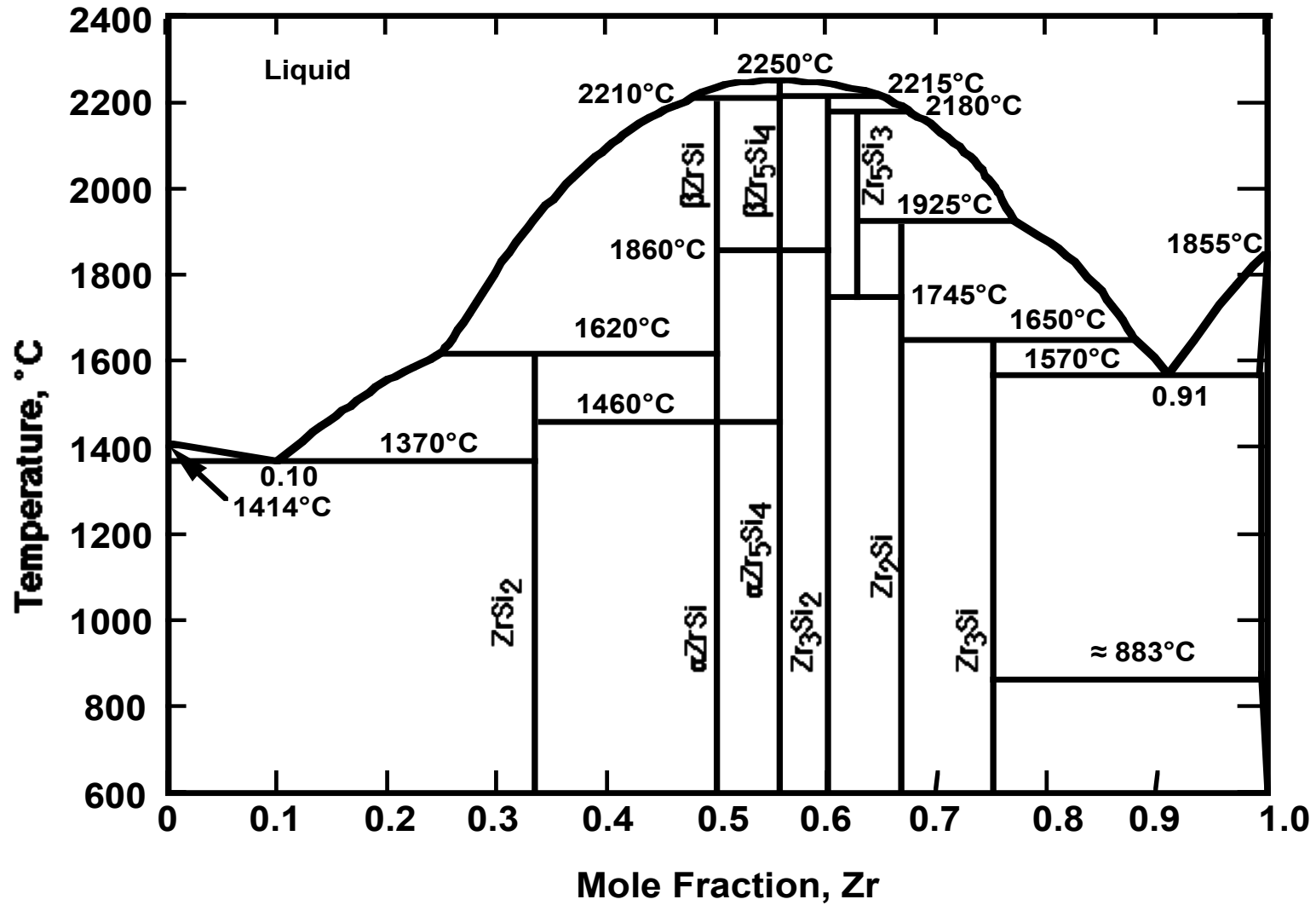


# Zr-C-B-Si Quaternary (Proposed by Sorrell-1993)



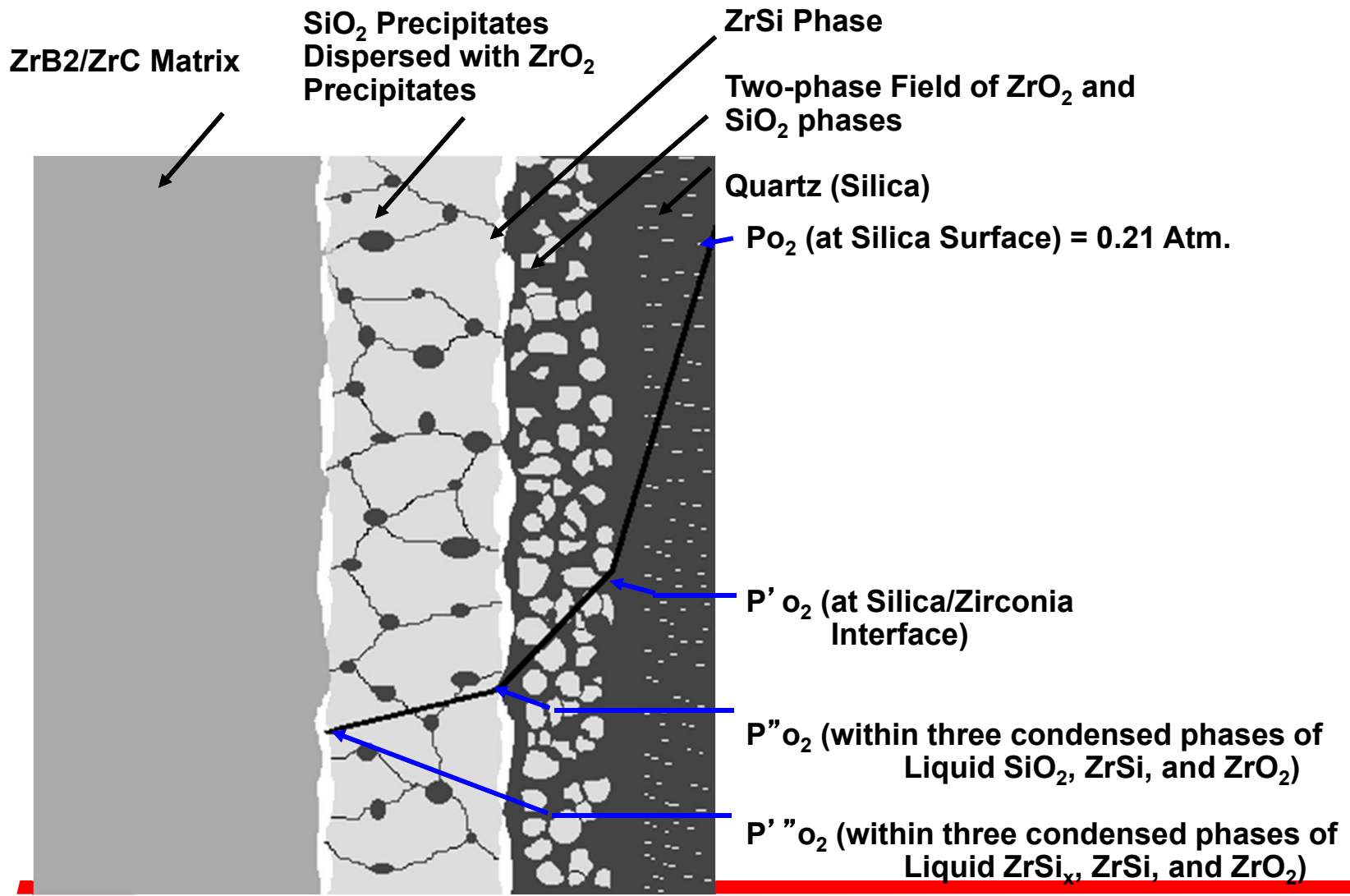


# Zr-Si Phase Diagram





# Oxygen Partial Pressure Gradient

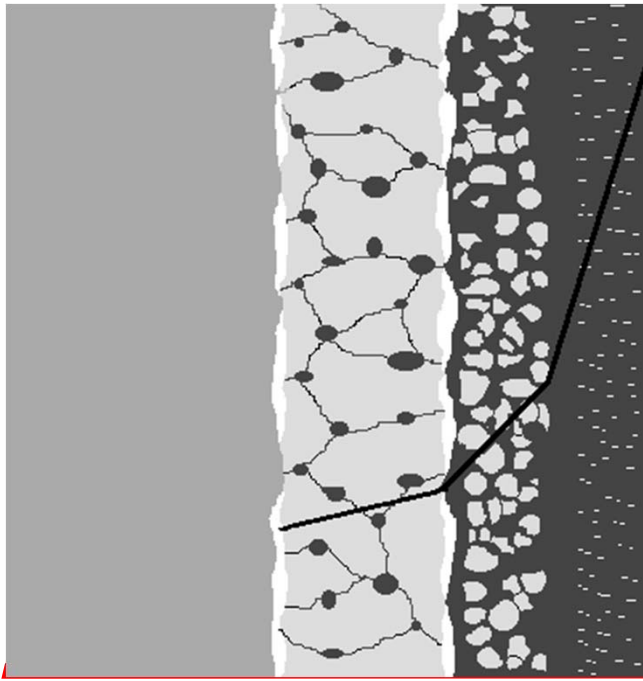


# Optimal Configuration of $ZrO_2$ Precipitates in $SiO_2$ Matrix

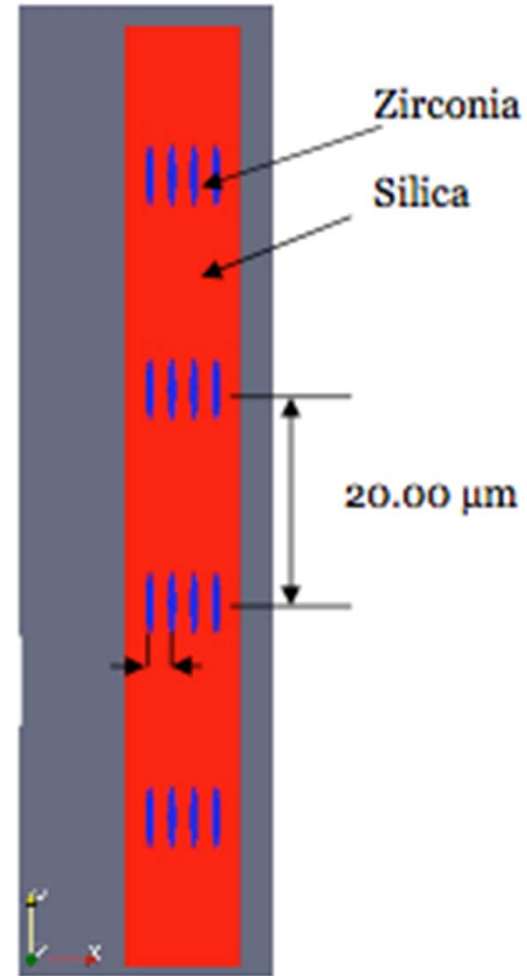
ZrC-ZrB<sub>2</sub>-  
Zr Matrix

ZrO<sub>2</sub>-SiO<sub>2</sub>  
Layer

SiO<sub>2</sub>-ZrO<sub>2</sub>  
Scale

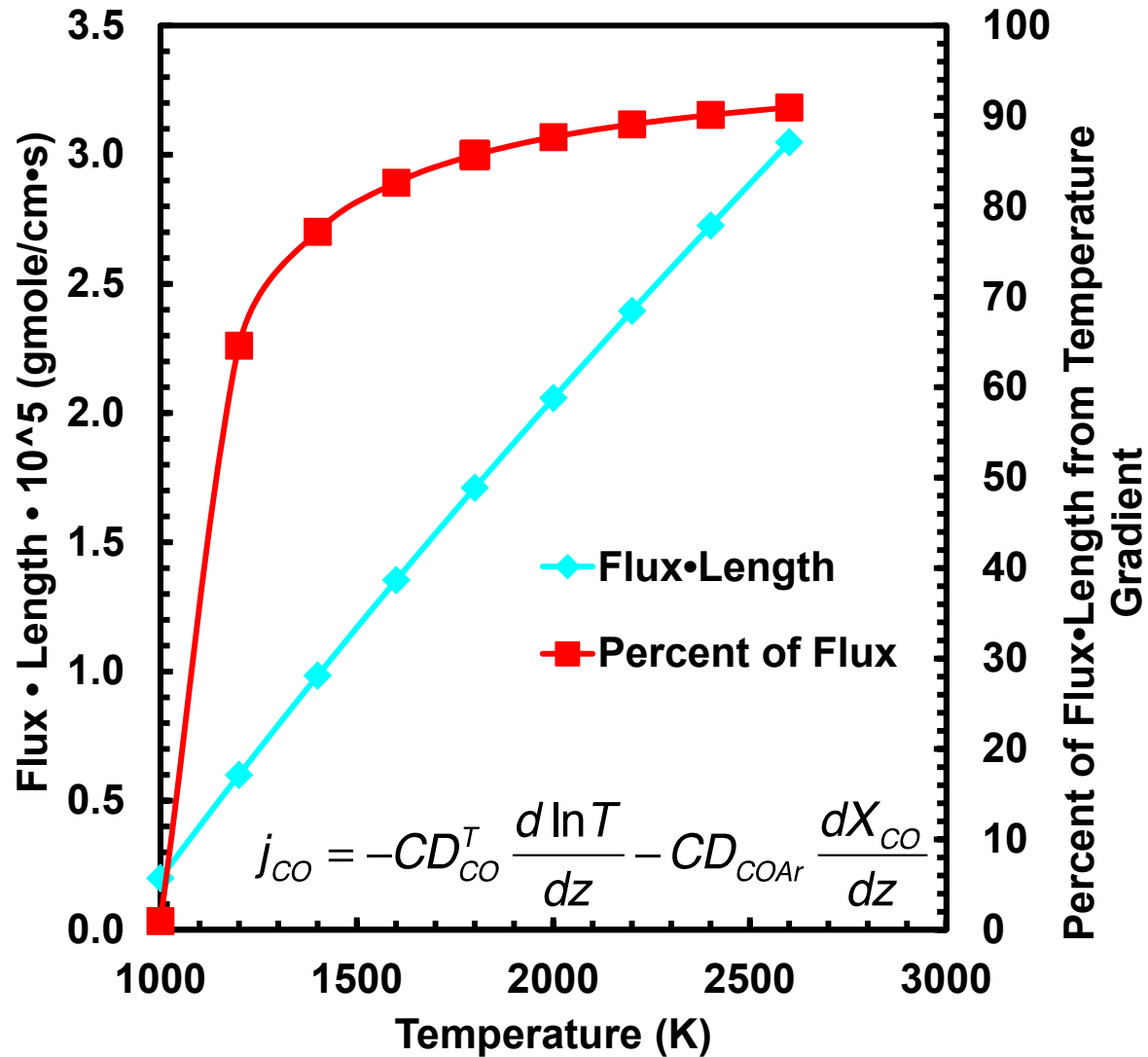


1.96  $\mu\text{m}$





# Diffusional Flux – Kinetics Issues



□  $D_{COAr}$  from Poirier-Geiger and checked with Chapman-Enskog Eq.

□ Mean temperature

$$\frac{T_H T_C}{T_H - T_C} \ln \frac{T_H}{T_C} = 1527K$$

□ Al/Al<sub>2</sub>O<sub>3</sub>/Al<sub>4</sub>CO<sub>4</sub> reaction rate?







# Surface Energies for Hf Alloy Melts Determined from Elements

